NRL Report 7080

Radiative Corrections to Electron Scattering From Complex Nuclei

H. Überall

Department of Physics
The Catholic University of America

and

NRL Linac Branch
Nuclear Physics Division

May 1, 1970

NAVAL RESEARCH LABORATORY
Washington, D.C.

Contents

Foreword

The following material has been prepared as part of a forthcoming book, Electron Scattering from Complex Nuclei, to be published by Academic Press, Inc., hopefully in 1970. The chapter on radiative corrections forms a self-contained entity, which might be of interest to experimental physicists working in the field of elastic or inelastic electron scattering, and for whom radiative corrections represent a matter of practical importance. For this reason, a separate publication of this single chapter as a Naval Research Laboratory Report apart from the book itself, and before its eventual publication, seemed to be warranted.

Occasionally, there appear references to equations contained in earlier chapters of the manuscript of the book. In the present report, these equations are collected in an Appendix.

We use this opportunity for requesting readers of this report to communicate to us any errors or need for clarifications they might discover, so that corresponding corrections may be made in the manuscript of the book before its publication.

Abstract

In this report, we give a review of the present status of radiative corrections to electron scattering from complex nuclei, both from the theoretical standpoint and with a view to practical applications. The first section presents a description of the general features of radiative corrections. The following four sections discuss the individual processes entering into radiative and line shape corrections and their synthesis, while the rest of the report is concerned with individual processes contributing to the radiation tail, and their synthesis (or "unfolding procedure").

Problem Status

This is an interim report on a continuing problem.

Authorization

NRL Problem: H01-09

Project: RR 002-06-41-5005

Manuscript submitted: February 24, 1970.

RADIATIVE CORRECTIONS TO ELECTRON SCATTERING FROM COMPLEX NUCLEI

7.2.1. GENERAL FEATURES OF RADIATIVE CORRECTIONS

The only major drawback in the use of the electron as a probe of nuclear structure is the fact that due to its small mass, it may be very easily deflected, and most of such deflections are accompanied by radiation. These radiation effects and related ionization effects, necessitate important corrections in the analysis of electron scattering experiments. They may be grouped into the following categories: (1) radiation effects during the scattering by the nucleus, (2) radiation and electronic collisions before or after scattering, and (3) straggling due to ionization effects. These shall now be discussed individually.

(1) Radiation effects during scattering. While the electron scatters off a given nucleus, it will at the same time interact with the radiation field emitting real and virtual photons, and the existence of these processes will modify the scattering cross section. The corresponding corrections might be referred to as "t-effects" since they are, just as the counting rate from the scattering process itself, proportional to the target thickness t. Two corrections appear:

(a) The Schwinger correction (Schwinger 49, 49b) which arises from the emission and reabsorption of virtual photons by the electron, and from the emission of soft, unobserved real photons. Its effect consists essentially in the multiplication of the scattering cross section $d\sigma/d\Omega$ by a correction factor

$(1 - \delta_s)$ with $\delta_s > 0$, so that

$$(d\sigma/d\Omega)_{obs} = (d\sigma/d\Omega)(1 - \delta_s). \tag{7.1}$$

One may thus either calculate the elastic cross section $d\sigma/d\Omega$ theoretically using a model, multiply by $(1 - \delta_s)$ and compare with the measured elastic peak, $(d\sigma/d\Omega)_{obs}$; or one may divide the measured peak $(d\sigma/d\Omega)_{obs}$ by $(1 - \delta_s)$ and use the resulting increased peak size for a comparison with the theoretical cross section $d\sigma/d\Omega$. Since the measured elastic peak has a tail toward the low-energy side, see Fig. 7.4, a cut-off at some energy ΔE, typically 1-2% below the peak energy, has to be made whose magnitude enters in the radiative correction. The correction δ_s is often fairly large, of the order of 20-30%. The correction procedure for electrons other than in the elastic peak is more involved, see below.

(b) The radiative tail (Racah 34, Schiff 52, McCormick 56) which consists of electrons that have emitted a hard photon during the scattering process, and whose energy has thus been degraded below the cutoff ΔE of the elastic peak. The form of the spectrum plotted vs. E_2 of these radiation-degraded electrons is typically as indicated in Fig. 7.4, showing first a decreasing tail extending below the elastic peak, which for very low electron energies rises up again (this will be understood later on). It is interesting to note for $\theta = 180^\circ$ scattering by a spinless nucleus that although the elastic peak

is here practically absent for all energies $E_1 \gg m_c$, it still gives rise to a radiation tail which now is monotonically increasing as the energy of the scattered electron E_2 decreases. A theoretical expression for the radiation tail is obtained essentially by integrating the Bethe-Heitler formula (Bethe 34, Heitler 54), or its generalization, for the emission of one bremsstrahlung photon over the directions of the unobserved photon.

Fig. 7.4 shows examples of inelastic peaks sitting on top of the radiation tail of the elastic peak; their area can be known only if the tail is subtracted accurately. As a matter of fact, each inelastic peak has its own (generally short) radiation tail, as illustrated in Fig. 7.5 for the scattering of 70 MeV electrons from ^{89}Y at $\vartheta = 130^{\circ}$ (Peterson 68). The area of a higher-energy excited level is determined by subtracting from the measured peak the radiation tail of the elastic peak and of all lower-lying excited levels (excitation energy increasing to the left of the figure).

(2) Radiation and electronic collisions before and after scattering.

(a) Radiation. The observed electron scattering may take place at one given nucleus, while emission of radiation may occur when the electron passes a different nucleus, either before or after the scattering. (One often neglects as small to second order those events where the electron emits radiation

successively in the field of several nuclei, including the scattering nucleus, since typical target thicknesses are 0.1 radiation length or less. In other words, the various corrections may then be applied additively.). The corresponding corrections might be referred to as "t^2-effects" since they depend on the target thickness to higher order than linearly, in general as the second power or higher (Nguyen Ngoc 65). The consequence of this radiation effect is just to add another contribution to the radiative tail mentioned above, as it also leads to a degradation of the scattered electron in energy. But it also leads to a broadening of the elastic and inelastic peaks.

(b) Electronic collisions. Another t^2-effect is the loss of energy of the electron (before or after scattering) by a collision with an atomic electron. Theoretically, this may be calculated using the formula of Møller (32) for electron-electron scattering, and the effect simply adds to the radiation tail.

By performing experiments with different target thicknesses the t and t^2 effects may be separated (Bounin 61), but this procedure is too lengthy for general use, and one resorts to calculations which are based on the Bethe-Heitler formula for (2a), and the Møller formula for (2b).

(3) Straggling due to ionization effects. The atomic ionizations which the electron, like any charged particle, gives rise to when traversing a target of finite thickness, lead to a large number of very small individual energy losses which are statis-

tically independent. The total energy loss is thus subject to statistical fluctuations which cause a broadening in energy of any originally monochromatic beam passing through the target, Gaussian in shape but with a tail toward the low-energy end. This phenomenon may be analyzed using the theories of Landau (44), or of Blunk and Leisegang (Blunk 50), and it leads to a broadening of the observed peaks in addition to the instrumental broadening which is present due to any original non-monochromaticity of the incident beam, or to finite energy resolutions of the counters. Another broadening is caused by the effect (2a) mentioned above ("radiation straggling").

The effects discussed above give rise to two different types of corrections of the experimental spectrum of scattered electrons before it can be theoretically interpreted (Nguyen Ngoc 65):

(A) Line shape correction. A given observed peak (with experimental cutoff ΔE) does not directly represent the entire corresponding cross section since the cross section is modified, and since some ot the electrons scattered at this energy are subsequently degraded in energy (and hence are not counted in the peak) by effects (1) - (3). The correction thus increases the experimental intensity $(d\sigma/d\Omega)_{obs}$, cf. (1a).

(B) Radiative tail correction. For inelastically scattered electrons, corresponding e.g. to a peak at energy $E_2 < E_1$, a spurious background is added to the observed intensity by the radiation tail of the lower excited levels or of the elastic peak, as shown above. This background must be calculated and subtracted from the peak; the corresponding subtraction is in general larger than the increase in intensity for the given peak provided by correction (A), so that a net decrease results. This is illustrated in Fig. 7.6 for scattering of 70 MeV electrons from ^{16}O (contained in H_2O) at $\vartheta = 180^\circ$ (Goldemberg 66). An elastic peak is present from ^{16}O $(J=0)$ due to the finite acceptance angle of the spectrometer, and from ^1H (displaced by recoil) due to its spin $J = \frac{1}{2}$. The (^{16}O ground state) radiation tail is indicated as a dashed line, and the corrections to the data (triangles) increase the elastic peaks corresponding to (A), while the inelastic peaks are decreased due to the combined effect of (A) and (B).

We shall now discuss the individual corrections quantitatively.

7.2.2. THE SCHWINGER CORRECTION

The question of the radiative corrections to electron scattering caused by virtual photons has received considerable theoretical attention since it is closely connected to a basic problem of quantum electrodynamics, namely the so-called "infrared catastrophy." This has to do with a divergence of the electrodynamic corrections to scattering processes which contain a term proportional to an integral over the energy k of the virtual photons,

$$\int_0^{\mathcal{E}} dk/k \ , \qquad (7\text{-}2a)$$

$\mathcal{E}$ being an upper limit above which the correction becomes negligible (Lomon 56). This integral diverges at the lower limit. A finite value is obtained if the photons are cut off at a small lower limit of their energy k_{min}. Alternately, in a covariant treatment, one may assign the photon a small rest mass Λ, but one obtains a similar divergence in the limit $\Lambda \to 0$.

All this can be described by perturbation theory in quantum electrodynamics, so that for the case of electron scattering, contributions of the diagrams shown in Fig. 7.7 must be evaluated. Diagram (a) alone leads to the Mott cross section, Eq. (2-70a), of order $(Ze^2)^2$. The interference terms between diagram (a) and diagrams (a') to (d') furnish the corrections of order $(Ze^3)^2$. Diagrams (a') to (c') describe the emission and reabsorption of virtual photons; of these, the electron self energy diagrams (a') and (b') lead to a mass and electron wave function renormalization (see, e.g., Jauch 55, Bjorken 65). Diagram (c') is called the vertex renormalization diagram; it cancels out the wave function renormalization of (a') and (b') by Ward's identity (Ward 50). Diagram (d') is the "vacuum polarization" (photon self energy) diagram which modifies the photon propagator, partly renormalizing the electron charge.

After carrying out the standard renormalization procedure using a small photon mass λ, both the self energy diagrams (a'), (b') and the vertex part (c') exhibit the mentioned infrared divergence (Karplus 50). This does not mean, however, that quantum electrodynamics fails when it comes to calculating radiative corrections. Schwinger (49b) has shown that if this theory is used to describe the electron scattering experiments as they are carried out in practice, the divergence will not arise. In any such experiment, the elastic scattering process will be indistinguishable from a process in which a soft real photon (of energy

$k < \Delta E$) is emitted during scattering: the finite energy resolution (of width ΔE) present in all the counters will cause the two types of scattering events to be lumped together. One therefore has to include in the cross section (and radiative correction) calculation the diagrams (a) and (b) of Fig. 7.8 in which one soft real bremsstrahlung photon is emitted by the electron.* The cross section corresponding to bremsstrahlung emission, of order $(Z \alpha^3)^2$ just as the radiative corrections, must be added incoherently to the scattering cross section obtained from all the diagrams of Fig. 7.7. It turns out that when integrating over the energies of the unobserved photons in the bremsstrahlung cross section, the same divergent integral

$$\int_0^{\Delta E} dk/k \qquad (7\text{-}2b)$$

is obtained, which exactly cancels that of Eq. (7.2a) to leave us with a finite correction containing the integral

---

*Diagrams (a') and (b') in Fig. 7.8 are less important, leading to a contribution to the corrections of relative order q/M, M = nuclear mass (Drell 52). For the important case of electron-proton scattering, they were taken into account together with the diagrams, analogous to those in Fig. 7.7, where virtual photons are attached to the proton line. The corresponding radiative corrections to electron-proton scattering (Tsai 61, Meister 63) have been reviewed by Mo and Tsai (Mo 69). For a calculation of electron-proton bremsstrahlung (Berg 58, 61; Isaev 59, 60), all four diagrams of Fig. 7.8 were used.

$$\int_{\Delta E}^{\varepsilon} dk/k \,. \qquad (7\text{-}2c)$$

This was first noticed by Braunbek and Weinmann (Braunbek 38) and by Bethe and Oppenheimer (Bethe 46).

The divergent integral of Eq. (7-2b) describing the emission of a single bremsstrahlung photon represents the original "infrared catastrophy", seemingly predicting an infinite total cross section of bremsstrahlung emission. Bloch and Nordsieck have shown, however (Bloch 37; see also Pauli 38) that for soft photons the first-order perturbation theory used in the derivation becomes inadequate; they were able to extend (in the soft-photon limit) perturbation theory to all orders, i.e. to any number of emitted photons, with the result that the infrared divergence disappears from the cross section, and that the probability for emission of a finite number of soft photons (including no photon!) in the scattering process is exactly zero, so that every such process is necessarily accompanied by an infinite number of soft photons (though of finite total energy).

This shows that there is no such thing as purely elastic scattering. Photons have no mass and are thus very easily shaken off. Alternately viewed, the Coulomb field accompanying a fast electron is transverse due to Lorentz contraction; when the electron changes direction during scattering, this field must readjust to the new direction, and the difference between the old

and the new field appears as radiation.

We thus see that for soft photons, all orders of perturbation must be taken into account. The same is true in the radiative corrections due to virtual photon, and Jauch and Rohrlich (Jauch 54; see also Kinoshita 50, Baumann 53) were able to show, using the methods of Bloch and Nordsieck, that the infrared divergences cancel out to all orders between the real and the virtual processes.

In the following, we shall sketch this cancellation in first order, and then quote the complete result for the radiative correction δ including emission of soft photons $k < \Delta E$. The lowest-order S-matrix is

$$S = -i \int \mathcal{H}_I \, d^4x = -e_0 \int d^4x \, \bar{\psi}_2 \gamma_\mu \psi_1 A_\mu(x), \qquad (7\text{-}3a)$$

where we used the symbol e_0 for the bare (unrenormalized) charge of the electron; the interaction Hamiltonian $\mathcal{H}_I$ follows e.g. from Eq. (2-25b). We assume a static Coulomb potential

$$A_\mu(x) = i\Phi = i\,\delta_{\mu 4}\, Ze/r \qquad (7\text{-}3b)$$

with Fourier transform

$$A_\mu(\Delta) = 2\pi i\,\delta(E)\,\delta_{\mu 4}\,(4\pi Ze/q^2) = 2\pi i\,\delta(E)\,\delta_{\mu 4}\,\Phi(q), \qquad (7\text{-}3c)$$

using the four-momentum transfer $\Delta = (q, iE)$. The S-matrix, from Eq. (7-3a), becomes

$$S(\underset{\sim}{k_1},\underset{\sim}{k_2}) = -e_0\,\bar{u}(\underset{\sim}{k_2})\,\gamma_\mu\,u(\underset{\sim}{k_1})\,A_\mu(\Delta)$$
$$= -e_0\,S_\mu\,A_\mu(\Delta), \qquad (7\text{-}3d)$$

with S_μ given by Eq. (4-2d). If now the renormalization is carried out (see, e.g., Jauch 55), the vertex $e_0\gamma_\mu$ including its radiative corrections given by the diagrams of Fig. 7.7, becomes

$$e_0\gamma_\mu \rightarrow e_e\left\{\gamma_\mu F_E(\Delta^2) + (\mu_e^a/2m_e)\,\sigma_{\mu\nu}\Delta_\nu F_M(\Delta^2)\right\}, \qquad (7\text{-}3e)$$

with the renormalized electron charge $e_e^2 = \alpha$. It is recognized that the radiative corrections have introduced an electric form factor $F_E(\Delta^2)$, and have added an anomalous magnetic moment of the electron with form factor $F_M(\Delta^2)$, of Eq. (3-37b). If we write

$$F_E(\Delta^2) = F_E'(\Delta^2) - \Delta^2\,\Pi(\Delta^2), \qquad (7\text{-}4a)$$

the contribution due to the vacuum polarization is obtained as

$$-\Delta^2\Pi(\Delta^2) = (2\alpha/\pi)\int_0^1 x(1-x)\ln\left[1+(\Delta^2/m_e^2)x(1-x)\right]dx, \qquad (7\text{-}4b)$$

with the limits

$$\Delta^2 \ll m_e^2, \quad -\Delta^2\Pi(\Delta^2) \rightarrow (\alpha/15\pi)(\Delta^2/m_e^2), \qquad (7\text{-}4c)$$

$$\Delta^2 \gg m_e^2, \quad -\Delta^2\Pi(\Delta^2) \rightarrow (\alpha/3\pi)\ln(\Delta^2/m_e^2). \qquad (7\text{-}4d)$$

The magnetic form factor, provided by diagram c' of Fig. 7.7, is given by

$$\mu_e^a F_M(\Delta^2) = \frac{\alpha}{\pi}\int_0^1 dx \int_0^x dy \; \frac{x(1-x)}{x^2+(\Delta^2/m_e^2)y(x-y)} \quad . \tag{7-4e}$$

In the limit $\Delta^2 \ll m_e^2$, it goes over into

$$F_M(\Delta^2) \to 1, \qquad \mu_e^a = \alpha/2\pi, \tag{7-4f}$$

i.e. into the static anomalous magnetic moment of the electron as first derived by Schwinger (48, 49b). The infrared divergence appears in the electric form factor: using the modified photon propagator of Eqs. (3-37c, d), one finds

$$F_E'(\Delta^2) = 1 - \frac{\alpha}{2\pi}\int_0^1 dx \int_0^x dy \left\{ \ln\left[1 + \frac{(\Delta^2/m_e^2)y(x-y)}{x^2+(\Lambda^2/m_e^2)(1-x)}\right] + \frac{\Delta^2}{m_e^2}\frac{(1-x+y)(1-y)}{x^2+(\Lambda^2/m_e^2)(1-x)} + 2(1-x-\tfrac{1}{2}x^2)\left[\frac{1}{x^2+(\Lambda^2/m_e^2)(1-x)+(\Delta^2/m_e^2)y(x-y)} - \frac{1}{x^2+(\Lambda^2/m_e^2)(1-x)}\right]\right\}, \tag{7-4g}$$

with the limit

$$\Delta^2/m_e^2 \ll 1, \quad F_E'(\Delta^2) \to 1 - \frac{\alpha}{3\pi}\frac{\Delta^2}{m_e^2}\left(\ln\frac{m_e}{\Lambda} - \frac{3}{8}\right); \tag{7-4h}$$

this illustrates the divergence for $\Lambda \to 0$, which also appears in the cross section for Coulomb scattering. The latter is given by

$$d\sigma = \frac{E_1}{k_1}\frac{m_e^2}{E_1 E_2}\left|S(\underset{\sim}{k}_1, \underset{\sim}{k}_2)\right|^2 \frac{d^3k_2}{(2\pi)^3} \tag{7-5a}$$

which, with Eqs. (7-3a, c), agrees with the previous expression Eq. (2-60a), and can be calculated using $S(k_1, k_2)$ of Eq. (7-3d), with the renormalization given in Eq. (7-3e). In the limit $\Delta^2/m_e^2 \ll 1$ or $\beta \ll 1$ which we here consider for purposes of illustration, the cross section is found as the Mott (or Rutherford) cross section modified by a factor,

$$\frac{d\sigma}{d\Omega} = \frac{d\sigma_R}{d\Omega}\left[1 - \frac{2\alpha}{3\pi}\frac{\Delta^2}{m_e^2}\left(\ln\frac{m_e}{\Lambda} - \frac{1}{5} - \frac{3}{8}\right)\right], \tag{7-5b}$$

if also the contribution of μ_e^a is disregarded; $d\sigma_R/d\Omega$ is given in Eq. (2-70d). Retaining the μ_e^a contribution will just remove the term 3/8.

As mentioned above, the cross section due to soft bremsstrahlung, i.e. diagrams (a) and (b) of Fig. 7.8, has to be added in order to cancel the logarithmic divergence $\ln(m_e/\Lambda)$ as $\Lambda \to 0$. For the emission of a photon with momentum k and polarization four-vector ε_λ, one has the interaction amplitude, using standard techniques:

$$S(k_1; k_2, k) = -e^2\left(\frac{4\pi}{2\omega_k}\right)^{1/2}\bar{u}(k_2)\left[\varepsilon_\lambda\gamma_\lambda\frac{1}{(k_2+k)_\nu\gamma_\nu - im_e}\gamma_\mu + \gamma_\mu\frac{1}{(k_1-k)_\nu\gamma_\nu - im_e}\varepsilon_\lambda\gamma_\lambda\right]u(k_1)A_\mu(\Delta). \tag{7-6a}$$

Here, $\omega_k = (k^2 + \Lambda^2)^{1/2}$ if the photon mass Λ is introduced again; the momentum transfer is $\Delta = k_1 - k_2 - k$. Rationalizing denominators and using Eqs. (2-33c, d) and (2-20c), we may rewrite

$$S(k_1; k_2, k) = -e^2\left(\frac{4\pi}{2\omega_k}\right)^{1/2} \bar{u}(k_2)\left[\left(\frac{\varepsilon\cdot k_2}{k\cdot k_2} - \frac{\varepsilon\cdot k_1}{k\cdot k_1}\right)\gamma_\mu + \frac{\varepsilon_\lambda \gamma_\lambda k_\nu \gamma_\nu}{2k\cdot k_2}\gamma_\mu + \gamma_\mu \frac{k_\nu \gamma_\nu \varepsilon_\lambda \gamma_\lambda}{2k\cdot k_1}\right] u(k_1) A_\mu(\Delta). \quad (7\text{-}6b)$$

For present purposes where only soft photons are considered, we shall just retain the first term in square brackets, which diverges as $k \to 0$, and which gives the infrared catastrophy, neglecting the two other (finite) terms compared to the first. One then has the covariant, gauge invariant expression

$$S(k_1; k_2, k) \cong -e^2\left(\frac{4\pi}{2\omega_k}\right)^{1/2}\left(\frac{\varepsilon\cdot k_2}{k\cdot k_2} - \frac{\varepsilon\cdot k_1}{k\cdot k_1}\right) S_\mu A_\mu(\Delta). \quad (7\text{-}6c)$$

The cross section is given by

$$d\sigma_B = \frac{E_1}{k_1}\frac{m_e^2}{E_1 E_2}\left|S(k_1; k_2, k)\right|^2 \frac{d^3k_2}{(2\pi)^3}\frac{d^3k}{(2\pi)^3}. \quad (7\text{-}6d)$$

Since the electron spin dependence of Eq. (7-6c) is the same as that of Eqs. (7-3d, e) (neglecting μ_e^a), and as we may also assume $\Delta \cong k_2 - k_1$ for soft photons, we have as in Eq. (7-5b):

$$\frac{d\sigma_B}{d\Omega} = \frac{d\sigma^c}{d\Omega}\frac{\alpha}{4\pi^2}\sum_\lambda \int \frac{d^3k}{\omega_k}\left(\frac{k_2\cdot\varepsilon^{(\lambda)}}{k_2\cdot k} - \frac{k_1\cdot\varepsilon^{(\lambda)}}{k_1\cdot k}\right)^2; \quad (7\text{-}6e)$$

$d\sigma^c/d\Omega$ is given by Eq. (2-70a). Carrying out the angular integration and the summation over the photon polarizations λ, and considering elastic scattering with emission of soft photons only, $k_2 \cong k_1 \equiv k_e$, we obtain in the previous limit $\Delta^2/m_e^2 \ll 1$, $k_e^2 \ll 1$:

$$\frac{d\sigma_B}{d\Omega} = \frac{d\sigma_R}{d\Omega}\frac{\alpha}{\pi}\frac{\Delta^2}{m_e^2}\int_0^{\Delta E}\left(\frac{1}{\omega_k^2} - \frac{1}{3}\frac{k^2}{\omega_k^4}\right)k^2\,dk. \quad (7\text{-}6f)$$

This must now be integrated over photon energies up to the experimental energy resolution ΔE. The result is

$$\frac{d\sigma_B}{d\Omega} = \frac{d\sigma_R}{d\Omega}\,\frac{2\alpha}{3\pi}\,\frac{\Delta^2}{m_e c^2}\left(\ln\frac{2\Delta E}{\Lambda} - \frac{5}{6}\right). \qquad (7\text{-}6g)$$

Adding $d\sigma_B/d\Omega$ to the radiation-corrected cross section of Eq. (7-5b), including the μ_e^a contribution, one gets the total observed cross section from which Λ has disappeared:

$$\frac{d\sigma(\Delta E)}{d\Omega} = \frac{d\sigma_R}{d\Omega}\left[1 - \frac{2\alpha}{3\pi}\,\frac{q^2}{m_e^2}\left(\ln\frac{m_e}{2\Delta E} + \frac{5}{6} - \frac{1}{5}\right)\right]. \qquad (7\text{-}6h)$$

Thus, the corrected cross section may be written

$$\frac{d\sigma(\Delta E)}{d\Omega} = \frac{d\sigma_R}{d\Omega}\,(1-\delta_S), \qquad k_e^2 \ll m_e^2, \qquad (7\text{-}7a)$$

with the Schwinger correction

$$\delta_S \cong \frac{2\alpha}{3\pi}\,\frac{q^2}{m_e^2}\left(\ln\frac{m_e}{2\Delta E} + \frac{19}{30}\right), \quad k_e^2 \ll m_e^2 \qquad (7\text{-}7b)$$

(for elastic scattering). In the general case of elastic scattering from a point Coulomb potential, to lowest order in the interactions, one has the cross section for an electron of initial energy E_1 and final energy E_2 with $E_1 - \Delta E \leq E_2 \leq E_1$:

$$\frac{d\sigma(\Delta E)}{d\Omega} = \frac{d\sigma^c}{d\Omega}\,(1-\delta_S). \qquad (7\text{-}8a)$$

Schwinger's (49) derivation of δ_S contained errors, which were shown by Elton (52) to cancel, however. Detailed derivations of δ_S are given by Akhiezer (65), or by Källén (58). The complete expression for δ_S is also quoted in the review paper by Motz (64), with corrections given by Maximon (69); it is expressed in terms

of the Euler dilogarithm (or Spence function*)

$$L_2(x) = -\int_0^x \frac{\ln(1-y)}{y}\, dy . \qquad (7\text{-}8b)$$

In the case of high electron energies, $E_1 \gg m_e$, which is of interest here, the Schwinger correction becomes

$$\delta_S = \frac{2\alpha}{\pi}\left\{\left[\ln\frac{E_1}{\Delta E} - \frac{13}{12}\right]\left[\ln\frac{q^2}{m_e^2} - 1\right] + \frac{17}{36}\right.$$

$$\left. + \frac{1}{2}\left[\frac{1}{6}\pi^2 - L_2\left(\cos^2\tfrac{1}{2}\vartheta\right)\right]\right\}, \quad q^2 \gg m_e^2 . \qquad (7\text{-}8c)$$

For its separation into infrared, vacuum polarization, and vertex parts, see Mo (69). This correction, for typical energies $E_1 = 100$ MeV, $\Delta E = 0.5$ MeV and angles $\vartheta = 60°$ is fairly large, $\sim$ 20%.

The results given here refer to elastic scattering from a point Coulomb charge treated in first Born approximation only (and the radiative correction given in lowest order), neglecting recoil. Many applications however require a broader region of validity. The necessary extensions have recently been discussed by Maximon (69). They are:

(1) Schwinger correction for inelastic scattering. If a nuclear level of energy ω is excited in the scattering, δ_S

---

*This is a monotonically increasing function of x for $0 \le x \le 1$ with $L_2(0) = 0$, $L_2(1) = \pi^2/6$.

becomes (Meister 64, Maximon 67, 69) with $E_2 = E_1 - \omega$:

$$\delta_S = \frac{2\alpha}{\pi}\left\{\left[\ln\frac{(E_1E_2)^{1/2}}{\Delta E} - \frac{13}{12}\right]\left[\ln\frac{q^2}{m_e^2} - 1\right] + \frac{17}{36} + \frac{1}{4}\ln^2\frac{E_1}{E_2}\right.$$

$$\left. + \frac{1}{2}\left[\frac{1}{6}\pi^2 - L_2\left(\cos^2\tfrac{1}{2}\vartheta\right)\right]\right\}, \quad q^2 \gg m_e^2. \tag{7-8d}$$

This may be used for the line shape correction of inelastic peaks.

(2) Effect of extended charges, and of extended magnetic moments. For the elastic case, it was shown (Elton 55) that δ_S remains uninfluenced by a spatial extension of the nuclear charge, so that $d\sigma^C/d\Omega$ in Eq. (7-8a) just gets multiplied by the nuclear form factor. For inelastic scattering, similar remarks apply, except that the rapid variation of inelastic form factors may require precautions (Maximon 69). One may also use the same δ_S for magnetic scattering, see Sec. 6.1. This, however, is correct only for $q^2 \gg m_e^2$ (Maximon 69).

(3) Exponentiation. Under certain circumstances, we may have to take into account higher-order radiative corrections when calculating δ_S. Schwinger (49b) noticed that δ_S may exceed unity for small ΔE, necessitating a modification of Eq. (7-8a). He thus suggested replacing the factor $(1 - \delta_S)$ by $\exp(-\delta_S)$, as then $d\sigma(\Delta E)/d\Omega$ would vanish for the case of $\Delta E \to 0$ $(\delta_S \to \infty)$, i.e. no pure scattering without accompanying photon would exist, in agreement with Bloch and Nordsieck's result (Bloch 37).

Higher-order radiative corrections were calculated by Jauch (54), Lomon (56), Yennie and Suura (Yennie 57a), Eriksson (61), Yennie, Frautschi, and Suura (Yennie 61) and Perrin and Lomon (Perrin 65). It is shown in these works that for elastic scattering the dominant soft-photon part of δ_s, which contains* the resolution ΔE,

$$\delta(\Delta E) = (2\alpha/\pi)\left[\ln\left(q^2/m_e^2\right) - 1\right]\ln\left(E_1/\Delta E\right), \tag{7-8e}$$

indeed has to be exponentiated; but it is not known at present whether the same should be done with the remainder,

$$\delta' = \delta_s - \delta(\Delta E)$$
$$= \frac{2\alpha}{\pi}\left\{-\frac{13}{12}\left[\ln\frac{q^2}{m_e^2} - 1\right] + \frac{17}{36} + \frac{1}{2}\left[\frac{1}{6}\pi^2 - L_2\left(\cos^2\tfrac{1}{2}\vartheta\right)\right]\right\}. \tag{7-8f}$$

It is therefore suggested (Maximon 69) to correct the cross section by

$$\frac{d\sigma(\Delta E)}{d\Omega} = \frac{d\sigma^c}{d\Omega}\, e^{-\delta(\Delta E)}\,(1-\delta'); \tag{7-9a}$$

but it may be just as accurate to use

$$\frac{d\sigma(\Delta E)}{d\Omega} = \frac{d\sigma^c}{d\Omega}\, e^{-\delta_s}. \tag{7-9b}$$

---

*Strictly speaking, the true soft-photon contribution has the logarithmic term $\ln(m_e/\Delta E)$ in place of $\ln(E_1/\Delta E)$; cf. Maximon (69).

(4) Exact scattering cross section. So far, all consideration of radiative corrections were made treating the electron-nucleus interaction in first Born approximation only. Mitter and Urban (Mitter 54), Newton (55, 55a) and Chrétien (65) considered the electron-nucleus interaction in second order (and the radiation correction in lowest order); Mittleman (54) treated the potential in all orders for nonrelativistic electrons. Suura (55), however, was able to show for the Coulomb potential that the main term in the radiative correction due to one soft photon,

$$(2\alpha/\pi)\,\ln(E_1/\Delta E)\,\ln(q^2/mc^2) \tag{7-10}$$

remained the same in all orders of the Born approximation for the electron-nucleus interaction. Since this provides most of the correction, it is suggested (Maximon 69) to rewrite Eqs. (7-9) in the form

$$\frac{d\sigma(\Delta E)}{d\Omega} = \left(\frac{d\sigma}{d\Omega}\right)_{th} e^{-\delta(\Delta E)}\,(1-\delta'), \tag{7-11a}$$

or alternately

$$\frac{d\sigma(\Delta E)}{d\Omega} = \left(\frac{d\sigma}{d\Omega}\right)_{th} e^{-\delta_S}, \tag{7-11b}$$

where $(d\sigma/d\Omega)_{th}$ is the theoretical cross section calculated exactly (e.g. by phase shift analysis), and to consider Eqs. (7-11a, b) a sufficiently accurate prescription for carrying out the radiative corrections.

(5) Recoil corrections. None of the preceding has taken

into account the recoil of the nucleus. The corresponding corrections fall into two groups: (a) kinematic effects given e.g. by the recoil factor of Eq. (2-13b), and (b) dynamic effects which may appear in the radiative corrections through the diagrams (a'), (b') of Fig. 7.8; cf. the footnote before Eq. (7-2b).

One kinematic effect to be considered is the fact that due to the nuclear recoil, electrons observed in the energy bin ΔE no longer correspond to photon energies $\leq \Delta E$: the photon energy now depends on the direction of its emission, and the limit of integration of the real-photon radiative correction must be modified accordingly.

The kinematic and dynamic corrections to electron scattering from a proton (of charge Ze) were calculated by Tsai (61), and by Meister and Yennie (Meister 63), and are reviewed and discussed in the paper by Mo and Tsai (Mo 69). Radiative corrections to electron-induced processes in which the final electron is not observed, were calculated by Kuo and Yennie (Kuo 66), and were found smaller than for comparable processes with a final electron detected.

7.2.3. THICK-TARGET BREMSSTRAHLUNG

Radiation straggling, which causes a broadening of the observed peaks, comes about by statistical fluctuations of small-energy bremsstrahlung losses in multiple collisions while the electron traverses a target of finite thickness. The probabi-

lity that an electron of initial energy E, after passing through a thickness t of matter, loses an energy between ε and $\varepsilon + d\varepsilon$ by radiation is given by* (Rossi 52)

$$P_{rad}(E,\varepsilon,t)\,d\varepsilon = \frac{d\varepsilon}{E}\,\frac{1}{\Gamma(t/x_0 \ln 2)}\left(\ln\frac{E}{E-\varepsilon}\right)^{\frac{t}{x_0 \ln 2}-1}, \quad (7\text{-}12a)$$

where X_0 is the radiation length. For $\varepsilon \ll E$, this may be written

$$P_{rad}(E,\varepsilon,t)\,d\varepsilon \cong \frac{d\varepsilon}{E\Gamma(t/x_0 \ln 2)}\left(\frac{\varepsilon}{E}\right)^{\frac{t}{x_0 \ln 2}-1}. \quad (7\text{-}12b)$$

If one defines a bremsstrahlung correction factor due to all losses up to ΔE by

$$e^{-\delta_B} = \int_0^{\Delta E} P_{rad}(E,\varepsilon,t)\,d\varepsilon, \quad (7\text{-}12c)$$

one finds using $\Gamma(x) \to 1/x$ as $x \ll 1$:

$$\delta_B \cong \frac{t}{x_0 \ln 2}\ln\frac{E}{\Delta E}. \quad (7\text{-}12d)$$

This is recognized as a t^2-effect.

7.2.4. LANDAU STRAGGLING

Another t^2-effect which causes a broadening of the peaks is the ionization straggling, in which the multiple small energy losses come from atomic ionization. Landau (44) has performed an analysis of this effect, with the result: the probability

*Mo and Tsai (Mo 69) have given a more accurate expression for $P_{rad}(E,\varepsilon,t)$.

that an electron of initial energy E , after passing through a thickness t of matter, loses an energy between ε and $\varepsilon + d\varepsilon$ by ionization is given by the Laplace transform

$$P_{ion}(E,\varepsilon,t)\,d\varepsilon = (d\varepsilon/2\pi i)\int_{\sigma-i\infty}^{\sigma+i\infty} ds\, e^{s\varepsilon}\, P_{ion}(E,s,t) \tag{7-13a}$$

($\sigma > 0$), where

$$P_{ion}(E,s,t) = e^{-s\xi(1-C-\ln s\varepsilon')} . \tag{7-13b}$$

Here, C = 0.577... is the Euler-Mascheroni constant, ε' is defined by

$$\ln \varepsilon' = \ln \frac{(1-\beta^2)I^2}{2m_e\beta^2c^2} + \beta^2 , \tag{7-13c}$$

the atomic ionization potential is $I \cong 13.5\, Z\ eV$, and

$$\xi = \frac{2\pi N e^4 \rho}{m_e\beta^2c^2}\,\frac{\Sigma Z}{\Sigma A}\,t \cong 0.154\, t\,(gm/cm^2)\,\frac{\Sigma Z}{\Sigma A}\,MeV, \tag{7-13d}$$

where N= Avagadro's number, ρ = density of matter, Z and A the atomic numbers and weights of the atoms in the molecule. This probability may be given in the form

$$P_{ion}(E,t,\varepsilon) = (1/\xi)\,\Phi(\lambda), \tag{7-14a}$$

in terms of a universal function $\Phi(\lambda)$ of the variable

$$\lambda = (\varepsilon - \varepsilon_0)/\xi \tag{7-14b}$$

where

$$\varepsilon_0 = \xi \left[\ln (\xi/\varepsilon') + 1 - C \right]. \qquad (7\text{-}14c)$$

The function $\Phi(\lambda)$ is given graphically in Landau's paper. It has an asymmetric peak* around $\lambda_{max} = -0.05$, so that the most probable energy loss is**

$$\tilde{\varepsilon} = \xi \left[\ln (\xi/\varepsilon') + 0.37 \right]$$

$$= \xi \left[\ln \frac{3 \times 10^3 \xi / \beta^2}{Z^2 (1-\beta^2)} + 1 - \beta^2 \right]. \qquad (7\text{-}14d)$$

The integrated energy loss

$$\int_0^{\Delta E} P_{ion}(E, \varepsilon, t)\, d\varepsilon = 1 - \Psi(\tilde{\lambda}), \qquad (7\text{-}15a)$$

$$\Psi(\tilde{\lambda}) = \int_{\Delta E}^{E} P_{ion}(E, \varepsilon, t)\, d\varepsilon \qquad (7\text{-}15b)$$

where $\tilde{\lambda} = (\Delta E - \varepsilon_0)\,\xi$, may be obtained from Landau's graph of the universal function $\Psi(\tilde{\lambda})$. For $\tilde{\lambda} < 10$, it can be fitted (Nguyen Ngoc 65) by

$$\Psi(\tilde{\lambda}) \cong \left[1.380 + 0.464\,\tilde{\lambda} + 0.024\,\tilde{\lambda}^2 \right]^{-1}, \qquad (7\text{-}15c)$$

---

*in such a way that a large energy loss may occur with significant probability. A tabulation is given by Börsch-Supan (61) which leads to a slightly different λ_{max}

**See also Sternheimer (52).

and for large arguments, approximate expressions are

$$\Psi(\tilde{\lambda}) \cong 1/\omega \qquad \tilde{\lambda} \geq 10 \tag{7-15d}$$

$$\Phi(\lambda) \cong 1/[\omega(\omega+1)], \qquad \lambda \geq 10. \tag{7-15e}$$

Here λ $(\tilde{\lambda})$ determines ω through the equation

$$\omega(\lambda) + \ln \omega(\lambda) = \lambda + 1 - C, \tag{7-15f}$$

which may be solved approximately by (Börsch-Supan 61)

$$\omega(\lambda) \cong \lambda \left(1 - \frac{\ln\lambda + C - 1}{\lambda + 1}\right). \tag{7-15g}$$

The correction factor due to all ionization losses up to ΔE is then approximately

$$\int_0^{\Delta E} P_{ion}(E, \varepsilon, t)\, d\varepsilon \cong \frac{\omega(\tilde{\lambda}) - 1}{\omega(\tilde{\lambda})} = 1 - J_I,$$

$$J_I = 1/\omega(\tilde{\lambda}). \tag{7-15h}$$

An earlier version of the theory of ionization straggling is due to Williams (29). Corrections to the Landau theory, taking into account resonance excitations, were given by Blunk and Leisegang (Blunk 50, 55); see also Breuer (65).

7.2.5. LINE SHAPE CORRECTION

The preceding information allows us to perform the radiative correction (A) of Sec. 7.2.1, i.e. either correcting the intensity of the line, or obtaining the shape of the line caused by

the radiative (t) and straggling (t^2) corrections.

If only the intensity correction is desired, one may in first approximation simply multiply the calculated cross section $d\sigma/d\Omega$ by the three correction factors listed above (Nguyen Ngoc 64),

$$\left(\frac{d\sigma}{d\Omega}\right)_{level} = \frac{d\sigma}{d\Omega}\, e^{-(\delta_S + \delta_B)}(1 - \delta_I). \tag{7-16}$$

What is the effective incident energy E_{eff} to be used both in the calculated cross section and in the correction factors? Statistically, the scattering takes place in the center of the target, so that the most probable straggling loss is $\frac{1}{2}\tilde{\varepsilon}$ (the most probable radiation straggling loss being zero), typically of the order of 100 keV. If E_{beam} is the energy of the electron beam as it is delivered by the accelerator, one has

$$E_{eff} = E_{beam} - \tfrac{1}{2}\tilde{\varepsilon}. \tag{7-17a}$$

After the electrons of energy E_{eff} scatter from a nucleus, the latter acquires a recoil energy T given by Eq. (2-12c), and possibly an excitation energy ω. A further ionization loss occurs when the electrons traverse the remainder of the target, so that the energy of the observed peak E_{pk} in the scattered electron spectrum is given by

$$E_{pk} = E_{eff} - \tfrac{1}{2}\tilde{\varepsilon} - T - \omega. \tag{7-17b}$$

In modern accelerators with good energy resolution, it will be necessary to obtain the complete line shape of the peaks as caused by the above described effects; in this case, the Schwinger, radiation, and Landau straggling effects must be folded into each other. If we consider the elastic peak ($\omega = 0$), say, and keep within its vicinity, so that $\frac{1}{2}\tilde{\varepsilon}$ is neglected in Eqs. (7-17), we may use a common energy $E_1 = E_{eff} \cong E_{beam} \cong E_{pk}$ (for a heavy nucleus, T is negligible also) for calculating the corrections. The folding is simplified by using the Laplace transforms (Bergstrom 67),

$$P(E_1, s) = \int_0^\infty P(E_1, \varepsilon)\, e^{-s\varepsilon}\, d\varepsilon , \tag{7-18a}$$

where $P(E_1, \varepsilon)$ is the folded probability distribution (i.e. the desired line shape) corresponding to incident energy E_1 and energy loss ε so that $E_2 = E_1 - \varepsilon$. We have from the folding theorem

$$P(E_1, s) = \int_0^{t_{1max}} P_{ir}(E_1, s, t_1)\, P_s(E_1, s)\, P_{ir}(E_1, s, t_2)\, dt_1 \tag{7-18b}$$

where t_1 (t_2) is the target thickness ahead (behind) the scattering nucleus, and

$$P_{ir}(E_1, s, t) = P_{ion}(E_1, s, t)\, P_{rad}(E_1, s, t) . \tag{7-18c}$$

Here, $P_{rad}(E_1, s, t)$ is the Laplace transform analogous to Eq. (7-13a). For the Schwinger correction, one differentiates

Eq. (7-11a) with respect to ΔE and takes the Laplace transform to obtain

$$P_S(E_1, s) = (1-\delta')\,\delta''\,\Gamma(\delta'')(E_1 s)^{-\delta''}\,d\sigma(E_1)/d\Omega, \tag{7-18d}$$

with

$$\delta'' = (2\alpha/\pi)\left[\ln(q^2/m_e^2) - 1\right]. \tag{7-18e}$$

A frequently used target arrangement is the so-called "transmission geometry" shown in Fig. 7.9, where the target is at a half-way angle between incident and scattered beam. This leads to

$$\begin{aligned} t_1 + t_2 \equiv t_{1\,max} &= const \\ &= t \equiv d/\cos\tfrac{1}{2}\vartheta, \end{aligned} \tag{7-18f}$$

no matter at which point inside the target the scattering took place. In this case, Eq. (7-18b) integrates easily, and one finds

$$P(E_1, s) = K \exp\left\{-T\ln s - s\xi\left[1 - C - \ln(s\varepsilon')\right]\right\}, \tag{7-18g}$$

where

$$T = \delta'' + t/\ln 2 \tag{7-18h}$$

(t being measured in radiation lengths), and

$$K = (1-\delta')\,\delta''\,\Gamma(\delta'')\,t\,E_1^{-T}\,d\sigma(E_1)/d\Omega. \tag{7-18i}$$

One may now perform the inverse Laplace transformation and close the contour as shown in Fig. 7.10. This leads to the line shape function (Bergstrom 67)

$$P(E_1, \Delta E) = K \xi^{T-1} I(\lambda, T) \tag{7-19a}$$

with λ defined in Eq. (7-14b), ξ given by Eq. (7-13d), and

$$I(\lambda, T) = \int_{c-i\infty}^{c+i\infty} e^{\lambda u - (T-u)\ln u}\, du, \tag{7-19b}$$

where $I(\lambda, 0) = \Phi(\lambda)$ of Eq. (7-14a). The Schwinger and radiation straggling effects enter into $I(\lambda, T)$ only through the combination T, in agreement with Bjorken's (63) conclusion. The observed cross section is then given by

$$\left(\frac{d\sigma(E_1)}{d\Omega\, d\epsilon}\right)_{line} = (1-\delta')\,\delta''\Gamma(\delta'')\left(\frac{d\sigma(E_1)}{d\Omega}\right)_{th} \frac{I(\lambda, T)}{E_1^T \xi^{1-T}}, \tag{7-19c}$$

which is the most general (differentiated) version of Eq. (7-11b). For describing inelastic peaks, the same expression may be used if the excitation energy is small, and the natural level width is much less than the Landau straggling width. Usually, $T < 0.1$, so that one may approximate (Bergstrom 67):

(a) if $\lambda \lesssim 10$,

$$I(\lambda, T) \cong \Phi(\lambda)\left[1 + (1+\lambda)T\right] + \tfrac{1}{2}T^2\left[\Psi(\lambda) - 1 + (1+\lambda)^2\,\Phi(\lambda)\right] \tag{7-19d}$$

with $\Phi(\lambda)$ and $\Psi(\lambda)$ the same as in Sec. 7.2.4;

(b) if $\lambda \gtrsim 10$,

$$I(\lambda, T) \cong \frac{\omega^T}{(1+\omega)^T \Gamma(T)}\left[T + \frac{1}{\omega} - \frac{8T}{\omega^2}\right], \tag{7-19e}$$

with ω determined by Eq. (7-15f). The first term in Eq. (7-19e) comes from Landau straggling, the rest from radiation effects, which latter thus dominate that part of the tail in the line shape where $\omega T > 1$.

Integrating Eq. (7-19c) over the line shape from $\varepsilon = 0$ to $\varepsilon = \Delta E$ gives, using Eq. (7-19e):

$$d\sigma(E_1)/d\Omega = e^{-\delta} \left[d\sigma(E_1)/d\Omega \right]_{th} \tag{7-20a}$$

with

$$e^{-\delta} \cong (1-\delta') \frac{\delta'' \Gamma(\delta'')}{T\Gamma(T)} \left(\frac{\omega \xi}{E_1} \right)^T \left[1 - \frac{1}{(1-T)\omega} \right]. \tag{7-20b}$$

Since $\delta'' \Gamma(\delta'') \cong 1$, $T\Gamma(T) \cong 1$, and for $\omega \gg 1$,

$$\omega \cong \lambda \cong \Delta E' / \xi , \tag{7-20c}$$

we obtain in this case (i.e. for $\lambda \gg 1$) again our previous Eq. (7-16), using $\Delta E' = \Delta E - \varepsilon_0$, i.e. measuring the cut-off energy from the maximum of the peak.

Fig. 7.11 shows the ratio

$$\frac{d\sigma(E_1)}{d\Omega\, d\varepsilon} \Big/ \left[\frac{d\sigma(E_1)}{d\Omega} \right]_{th} \tag{7-20d}$$

of Eq. (7-19c), obtained numerically and plotted vs. ε , for ^{208}Pb at $E_1 = 400$ MeV, $\vartheta = 90^{\circ}$ and for a target thickness $d = 30$ mg/cm^2. The T=0 curve shows the effect of Landau straggling only, the T = 1.04 x 10^{-2} curve the effect of Landau plus radiation straggling, and the T = 7.09 x 10^{-2} curve the

effect of all three corrections. The $\times$ indicates the $\omega T = 1$ position. If the scattering angle ϑ is increased, the line broadens according to

$$\Gamma \cong \Gamma_0 (1 + 2.06 T), \tag{7-20e}$$

where $\Gamma_0 = 3.98\,\xi$ is the Landau half-width, and the position of the peak shifts further away from the incident energy E_1.

7.2.6. HARD-PHOTON BREMSSTRAHLUNG

The radiation effects and corrections considered above modify the shape and the area of elastic and inelastic electron scattering peaks down to a cutoff-energy ΔE, usually taken as $\sim$ 1 MeV. The radiation tail that reaches from each peak all the way down to zero energy of the scattered electrons has to be calculated also, for the purpose of subtracting the background that it provides for the inelastic peaks. It again consists of t-effect and t^2-effect contributions, the latter from radiation and ionization before and after scattering, the former from the radiation of hard ($k > \Delta E$) photons during scattering. This effect will be considered here first.

The infinite number of photons emitted in the electron scattering process consists mainly of very soft photons for which lowest-order perturbation theory does not apply (Bloch 37). Hard-photon emission however can be treated in first Born approximation (for nuclei that are sufficiently light), and one

only needs to integrate the bremsstrahlung cross section over the directions of the unobserved single photon.

The bremsstrahlung cross section for a static Coulomb field (including screening, but not nuclear size) without recoil (Bethe 34, Heitler 54) has been integrated for the case of a point nucleus by Racah (34) and by McCormick (56), and the effect of a spherically symmetric nuclear charge distribution* was taken into account by a charge form factor in the work of Maximon and Isabelle (Maximon 64). To this has been added the contribution of a (spherically symmetric) magnetic moment** by Ginsberg and Pratt (Ginsberg 64); see also Motz (64), Goldemberg (66).

Schiff (52) has given a simple prescription for approximately carrying out the angular integration over photons. His "peaking approximation", frequently used by experimenters, e.g., in the results of Peterson (68) shown in Fig. 7.5, is based on the fact that for high energy electrons, bremsstrahlung is emitted mainly in a small cone of opening angle $m_e c^2/E_e$ around the direction of both incident and scattered electron. This reduces the cross section to a simple physically meaning-

---

*Nuclear size effects in bremsstrahlung have first been considered by Hough (48), and by Biel and Burhop (Biel 55).

**Magnetic moment contributions for bremsstrahlung were considered earlier by Sarkar (60) and by Dowling (64); for its effect on electron polarizations, see Kerimov (67).

ful expression (Friedman 59) consisting of* a term proportional to the elastic scattering cross section $d\sigma/d\Omega$ at energy E_1 (i.e. scattering before radiation), and a term with $d\sigma/d\Omega$ at energy $E_2 = E_1 - k$ (i.e. scattering after radiation). The validity of the peaking approximation has been examined by Maximon (64) and by Mo (69).

The bremsstrahlung cross section for the case that at the same time the nucleus is left in an excited state, has been derived by Perez y Jorba (61) using the peaking approximation. A more general calculation of the radiation tail of excited states has been performed by Maximon and Isabelle (Maximon 64a), in which the differential cross section is expressed by the same nuclear multipole form factors $F_C^2(q)$ and $F_T^2(q)$, Eqs. (4-16e, f), which also appear in the elastic Born cross section, Eq. (4-16c). This is a consequence of the fact, mentioned at the beginning of Section 4.1, that in any type of electrodynamic nuclear interaction with one-photon exchange, and no observation of the final nuclear states, the result always depends on the same two invariant functions (called W_1, W_2 in Section 4.1), no matter what goes on at the other end of the photon line. The cross section integrated over photon angles is left as an integral over dq^2 by Maximon and Isabelle.

*A form of the bremsstrahlung cross section given in terms of the elastic scattering amplitudes (and going beyond the Born approximation) has been derived by Parzen (51).

All the work mentioned above has neglected the recoil of the nucleus (except through a kinematic factor f_{rec}), often (but not always) also neglecting the electron mass m_e It is hence superseded* by a more general formula given by Tsai (Tsai 64, Mo 69) and by Nguyen Ngoc and Perez y Jorba (Nguyen Ngoc 64, 65), valid** for any target spin, arbitrary final (elastic or inelastic) unobserved nuclear (or nucleon) states, given in terms of the two general form factors W_1 and W_2 all with correct relativistic kinematics. A similarly general

*After an estimate of kinematic and dynamic recoil effects in the Bethe-Heitler formula was given by Drell (52), Berg and Lindner (Berg 58, 61) gave a completely relativistic formula for the radiation tail from the elastic peak of the proton, but with special assumptions for the form factors (equality of Dirac and Pauli form factor).

**Although photon emission from the nuclear system (the dynamic recoil effect) is accounted for in the form factors, it does lead to interferences with photons emitted by the electron line. Such interference terms are not taken into account in Tsai's and Nguyen Ngoc's formula. Further interference terms arise from photon decay of virtual excited nuclear levels; this effect has been considered by Hubbard (66) and by Acker (67), and will be discussed in Chapter 8 of this book.

result, but making use of the peaking approximation, is given by Meister and Griffy (Meister 64) and by Henry (66). Nguyen Ngoc's result was used in a recent calculation of the radiation tails (Bergstrom 67). But even these general formulas depend on the assumption of one-photon exchange; a usable calculation that goes beyond the first Born approximation does not yet appear in the literature*, even though such a result is clearly needed for obtaining radiative corrections that are reliable for more than just the lightest nuclei.

In the following, we shall sketch the derivation of Tsai's and Nguyen Ngoc's formula, and give their results.

Eq. (7-6d) gives the bremsstrahlung cross section in the laboratory system. For a general nuclear current rather than an external potential A_μ, the expression Eq. (7-6b) may be used in σ_B with the replacement ($\Delta = k_1 - k_2 - k$):

$$A_\mu(\Delta) \to (4\pi e/\Delta^2)(2\pi)^4 \delta^4(\Delta + P_1 - P_2)\langle P_2 | j_\mu(0) P_1\rangle, \quad \text{(7-21a)}$$

obtained by comparing Eqs. (7-5a) and (2-60a), and using Eq. (4-2e). Upon squaring $S(\underset{\sim}{k_1}, \underset{\sim}{k_2}, \underset{\sim}{k})$, one encounters the expression

$$S_{\mu\nu} = \frac{1}{2}\sum_{r_1 r_2 \lambda} \bar{u}(\underset{\sim}{k_1})\,\tilde{j}_\mu^{(e)}\,u(\underset{\sim}{k_2}).\,\bar{u}(\underset{\sim}{k_2})\,\tilde{j}_\mu^{(e)}\,u(\underset{\sim}{k_1}) \quad \text{(7-21b)}$$

(summed over spins and photon polarization), with

*A phase shift calculation of bremsstrahlung is now being performed (Onley 70).

$$\tilde{j}_{\mu}^{(c)} = \left(\frac{\varepsilon\cdot k_2}{k\cdot k_2} - \frac{\varepsilon\cdot k_1}{k\cdot k_1}\right)\gamma_\mu + \frac{\varepsilon_\lambda\gamma_\lambda k_\nu\gamma_\nu}{2k\cdot k_2}\gamma_\mu + \gamma_\mu\frac{k_\nu\gamma_\nu\varepsilon_\lambda\gamma_\lambda}{2k\cdot k_1}. \quad (7\text{-}21c)$$

This may be evaluated by the trace method of Section 2.3. Furthermore, one also obtains as a factor the tensor $W_{\mu\nu}$ of Eqs. (4-3a), (4-3c), expressed by two invariant functions W_1, W_2, which are related to the functions F, G of Nguyen Ngoc (64, 65) by

$$W_1 = (N_A N_B / P_{20})\, G(\Delta^2)\, \delta(\Delta_0 + P_{10} - P_{20}), \quad (7\text{-}21d)$$

$$W_2 = (N_A N_B / P_{20})\, M^2 F(\Delta^2)\, \delta(\Delta_0 + P_{10} - P_{20}); \quad (7\text{-}21e)$$

likewise, $W_{\mu\nu}$ is related to Nguyen Ngoc's tensor $T_{\mu\nu}$ by

$$W_{\mu\nu} = (N_A N_B / P_{20})\, T_{\mu\nu}\, \delta(\Delta_0 + P_{10} - P_{20}), \quad (7\text{-}21f)$$

$N_{A,B}$ being his normalization factors. The cross section may also be written in a general Lorentz system, where Eq. (4-3d) applies, and one has

$$\frac{d\sigma}{d\Omega\, dE_2} = \frac{\alpha^3}{(2\pi)^2}\frac{4m_e^2 k_2}{\left[(k_1\cdot P_1)^2 - m_e^2 M^2\right]^{1/2}}\int_{-1}^{1}\frac{k^2}{k\cdot P_2}\frac{d\cos\vartheta_k}{\Delta^4}\int_0^{2\pi} S_{\mu\nu}T_{\mu\nu}\, d\varphi_k, \quad (7\text{-}22a)$$

with (given here only in the laboratory* system again, $\underset{\sim}{P_1} = 0$):

*An expression for $S_{\mu\nu}T_{\mu\nu}$ in a general Lorentz system is given by Nguyen Ngoc (64, 65).

$$\int_0^{2\pi} S_{\mu\nu} T_{\mu\nu}\, d\varphi_k = (\pi M^2/m_e^2) N_A N_B F(\Delta^2) \{[2E_2(E_1-k) - \tfrac{1}{2}\Delta^2]$$

$$\cdot[-(\cos\vartheta_k - x_1)^2 + (m_e^2 x_1/kE_1)(\cos\vartheta_k - x_1) - (y_1^2/k)(E_1+k)]/(k k_1 \lambda_1^{3/2})$$

$$+[2E_1(E_2+k) - \tfrac{1}{2}\Delta^2][(\cos\vartheta_k - x_2)^2 + (m_e^2 x_2/kE_2)(\cos\vartheta_k - x_2)$$

$$-(y_2^2/k)(E_2-k)]/(k k_2 \lambda_2^{3/2}) - 2$$

$$-(2/k^2)(k_2^{-1}\lambda_2^{-1/2} - k_1^{-1}\lambda_1^{-1/2})[m_e^2(k_1\cdot k_2 + k^2) + k_1\cdot k_2\,(E_1E_2 + \underset{\sim}{k_1}\cdot\underset{\sim}{k_2}$$

$$+ k(E_1 - E_2))]/(E_1 - E_2 - |\underset{\sim}{u}|\cos\vartheta_k) + (m_e^2 - k_1\cdot k_2 - 2E_1^2)/(k k_1 \lambda_1^{1/2})$$

$$-(m_e^2 - k_1\cdot k_2 - 2E_2^2)/(k k_2 \lambda_2^{1/2})\}$$

$$+(\pi/m_e^2) N_A N_B G(\Delta^2)\{m_e^2(\Delta^2 - 2m_e^2)[(E_1^2 y_1^2 m_e^{-2}$$

$$- x_1(\cos\vartheta_k - x_1))/(k^2 k_1 E_1 \lambda_1^{3/2}) + (E_2^2 y_2^2 m_e^{-2} - x_2(\cos\vartheta_k - x_2))/(k^2 k_2 E_2 \lambda_2^{3/2})]$$

$$-4 - (\Delta^2 + 2m_e^2 + 6\,k_1\cdot k_2)(k_2^{-1}\lambda_2^{-1/2} - k_1^{-1}\lambda_1^{-1/2})/k$$

$$+4k^{-2}\,k_1\cdot k_2\,(\Delta^2 + k_1\cdot k_2)(k_2\lambda_2^{-1/2} - k_1\lambda_1^{-1/2})/(E_1 - E_2 - |\underset{\sim}{u}|\cos\vartheta_k)\}.$$

(7-22b)

The axes are chosen as

$$\hat{z} \parallel \underset{\sim}{k_1} - \underset{\sim}{k_2}\,, \qquad \hat{y} \parallel \underset{\sim}{k_1}\times\underset{\sim}{k_2}\,, \qquad \hat{x} = \hat{y}\times\hat{z}\,.$$

(7-22c)

For the photon energy, one has

$$k = \tfrac{1}{2}\,(M^{*2} + u^2) \,/\, (|\underset{\sim}{u}| \cos\vartheta_k - u_0), \tag{7-22d}$$

with the four-vector $u = k_1 - k_2 + P_1 = k + P_2$, and

$$\vartheta_k = \sphericalangle\,(\underset{\sim}{u}, \underset{\sim}{k}), \quad \varphi_k = \sphericalangle\,(\underset{\sim}{u}\,\underset{\sim}{k} \text{ plane}, \underset{\sim}{k_1}\,\underset{\sim}{k_2} \text{ plane}). \tag{7-22e}$$

Further notation is

$$x_i = E_i\, k_{iz} \,/\, \underset{\sim}{k_i}^2 \;, \quad y_i = m_e\, k_{ix} \,/\, \underset{\sim}{k_i}^2 \qquad (i = 1, 2) \tag{7-22f}$$

and

$$\lambda_i = (\cos\vartheta_k - x_i)^2 + y_i^{\,2} \,. \tag{7-22g}$$

In the integral of Eq. (7-22a), one may write

$$k \cdot P_2 = k \cdot u = -\,k\,(u_0 - |\underset{\sim}{u}| \cos\vartheta_k). \tag{7-22h}$$

Note that due to the recoil, the photon energy k depends on the direction of photon emission*, cf. Eq. (7-22d). These results show that, as stated before, bremsstrahlung may also be written in terms of the two invariant functions W_1 and W_2, or F and G. For practical calculations, it becomes of interest to express these functions by the multipole matrix elements, or equivalently, by the form factors $F_C^{\,2}(q)$ and $F_T^{\,2}(q)$ of Eqs. (4-16e, f) which enter in the cross section without photon emission, Eq. (4-16c). One finds neglecting recoil (but without

*Neglecting recoil, there is no such dependence since $u_0 \gg |\underset{\sim}{u}|$.

neglect of m_e):

$$N_A N_B G = 2\pi M P_{20} F_T^2(q), \tag{7-23a}$$

$$N_A N_B F = 4\pi (P_{20}/M)(\Delta^2/q^2)^2 \left[(\Delta^2/q^2) F_C^2(q) - \tfrac{1}{2} F_T^2(q)\right]. \tag{7-23b}$$

This also provides relations between the invariant functions appearing in the cross section without radiation of Section 4.1 and Section 4.2.

Without nuclear recoil, but taking nuclear excitation into account ($\omega \neq 0$), Maximon and Isabelle (Maximon 64a) have derived the differential bremsstrahlung cross section in terms of $F_C^2(q)$ and $F_T^2(q)$ as a special case of Eqs. (7-22). It is given in the form

$$\frac{d\sigma}{d\Omega\, dE_2} = \frac{\alpha^3}{(2\pi)^2} \frac{E_2 d\Omega_k}{k k_1} \left\{ \frac{4\pi}{q^4} F_C^2(q)\, \sigma_L + \frac{4\pi}{2(q^2-\omega^2)^2} F_T^2(q) \sigma_T \right\}, \tag{7-24a}$$

with $F_C^2(q)$, $F_T^2(q)$ as defined in Eqs. (4-16e, f), and where again

$$\underset{\sim}{q} = \underset{\sim}{k_1} - \underset{\sim}{k_2} - \underset{\sim}{k}, \tag{7-24b}$$

$$\omega = k_1 - k_2 - k; \tag{7-24c}$$

the functions σ_L , σ_T are given by Maximon (Eqs. 16, 17) for the general case $m_e \neq 0$. They contain the characteristic energy denominators of bremsstrahlung,

$$(E_1 - k_1 \cos\vartheta_1)^{-1}, \qquad (E_2 - k_2 \cos\vartheta_2)^{-1}, \tag{7-24d}$$

where $\vartheta_i = \sphericalangle(\underset{\sim}{k}_i, \underset{\sim}{k})$. If only Coulomb scattering is considered ($F_T \to 0$), Eq. (7-24a) reproduces the expression for the inelastic bremsstrahlung cross section obtained by Perez y Jorba (61).

Setting $\omega = 0$, one obtains from Eq. (7-24a) the expressions given by Ginsberg and Pratt (Ginsberg 64) for the elastic case:

$$\sigma_L(\omega=0) = \frac{(4E_2^2 - q^2)(\underset{\sim}{k}\times\underset{\sim}{k}_1)^2}{(kE_1 - \underset{\sim}{k}\cdot\underset{\sim}{k}_1)^2} + \frac{(4E_1^2 - q^2)(\underset{\sim}{k}\times\underset{\sim}{k}_2)^2}{(kE_2 - \underset{\sim}{k}\cdot\underset{\sim}{k}_2)^2}$$

$$+2\,\frac{k^2(\underset{\sim}{k}\times\underset{\sim}{k}_2)^2 + k^2(\underset{\sim}{k}\times\underset{\sim}{k}_1)^2 - (4E_1E_2 + 2k^2 - q^2)(\underset{\sim}{k}\times\underset{\sim}{k}_1)\cdot(\underset{\sim}{k}\times\underset{\sim}{k}_2)}{(kE_1 - \underset{\sim}{k}\cdot\underset{\sim}{k}_1)(kE_2 - \underset{\sim}{k}\cdot\underset{\sim}{k}_2)} \tag{7-24e}$$

which is familiar from the Bethe-Heitler formula, and

$$\sigma_T(\omega=0) = \frac{(4k_2^2 + q^2)(\underset{\sim}{k}\times\underset{\sim}{k}_1)^2}{(kE_1 - \underset{\sim}{k}\cdot\underset{\sim}{k}_1)^2} + \frac{(4k_1^2 + q^2)(\underset{\sim}{k}\times\underset{\sim}{k}_2)^2}{(kE_2 - \underset{\sim}{k}\cdot\underset{\sim}{k}_2)^2} + 4k^2\left(\frac{kE_1 - \underset{\sim}{k}\cdot\underset{\sim}{k}_1}{kE_2 - \underset{\sim}{k}\cdot\underset{\sim}{k}_2}\right.$$

$$\left. + \frac{kE_2 - \underset{\sim}{k}\cdot\underset{\sim}{k}_2}{kE_1 - \underset{\sim}{k}\cdot\underset{\sim}{k}_1}\right) + 2\,\frac{k^2(\underset{\sim}{k}\times\underset{\sim}{k}_2)^2 + k^2(\underset{\sim}{k}\times\underset{\sim}{k}_1)^2 - [4(E_1E_2 - m_e^2) + 2k^2 + q^2](\underset{\sim}{k}\times\underset{\sim}{k}_1)\cdot(\underset{\sim}{k}\times\underset{\sim}{k}_2)}{(kE_1 - \underset{\sim}{k}\cdot\underset{\sim}{k}_1)(kE_2 - \underset{\sim}{k}\cdot\underset{\sim}{k}_2)}. \tag{7-24f}$$

For spherically symmetric charge and magnetic moment distributions, one obtains using Eqs. (3-3f) and (4-27e):

$$\frac{d\sigma}{d\Omega\, dE_2} = \frac{Z^2\alpha^3}{(2\pi)^2}\,\frac{E_2\, d\Omega_k}{k k_1 q^4}\left\{\left[F_0^c(q)\right]^2\sigma_L(\omega=0) + \frac{J+1}{3J}\left(\frac{\mu}{Z}\right)^2\left(\frac{q}{2m}\right)^2\left[F_1^M(q)\right]^2\sigma_T(\omega=0)\right\}. \tag{7-24g}$$

Since in an electron scattering experiment the emitted photon is not observed, we integrate as before the general cross section Eq. (7-24a) over photon angles $d\Omega_k$. This is best transformed into an integration over ϑ_k and q^2, and one finds the cross section in the form of an integral over the form factors

$$\frac{d\sigma}{d\Omega dE_2} = \frac{2\alpha^3 E_2}{k k_1} \int_{q_m^2}^{q_M^2} \left\{ \frac{F_c^2(q)}{q^4} I_L(q^2) + \frac{F_T^2(q)}{2(q^2-\omega^2)^2} I_T(q^2) \right\} dq^2 \tag{7-25a}$$

where

$$q_m = |\underset{\sim}{k}_1 - \underset{\sim}{k}_2| - k, \tag{7-25b}$$

$$q_M = |\underset{\sim}{k}_1 - \underset{\sim}{k}_2| + k, \tag{7-25c}$$

and where the functions $I_L(q^2)$, $I_T(q^2)$ are given explicitly by Maximon (64a). In the elastic case ($\omega = 0$), they coincide with the corresponding functions R_{ch}, R_{mag},

$$I_L(\omega=0) = k R_{ch}, \quad I_T(\omega=0) = k R_{mag} \tag{7-25d}$$

of Ginsberg and Pratt (Ginsberg 64, Goldemberg 66); for spherically symmetric densities, one has further

$$\frac{d\sigma}{d\Omega dE_2} = \frac{Z^2\alpha^3 E_2}{2\pi k_1} \int_{q_m^2}^{q_M^2} \left\{ \left[F_0^c(q)\right]^2 R_{ch} + \frac{J+1}{3J} \left(\frac{\mu}{Z}\right)^2 \left(\frac{q}{2m}\right)^2 \left[F_1^M(q)\right]^2 R_{mag} \right\} \frac{dq^2}{q^4} \tag{7-25e}$$

For general form factors, the integrals in Eq. (7-25a) must be evaluated numerically. In the case of elastic scattering from nuclear point charges, i.e. the spherically symmetric

case with $F_0^d \to 1, F_1^M \to 1$, they may be performed analytically (Racah 34, McCormick 56, Ginsberg 64; see also Motz 64). Numerical examples will be presented below.

In most experiments of interest, the high-energy limit $(E_1, E_2 \gg m_e)$ applies. In this case, the approximation of Schiff (52), or "peaking approximation", permits the integration in Eqs. (7-25) to be carried out for general form factors. The basis for this is the observation that the denominators of Eqs. (7-24d) render the cross section large if the photon is emitted predominantly along the direction of the incident or of the scattered electron. In q-space, the peaks of the corresponding terms (after the ϑ_k -integration) are located at

$$q = q_i \equiv 2k_i \sin\tfrac{1}{2}\vartheta \,, \tag{7-26a}$$

i.e. at values of q that correspond to radiationless elastic scattering with electron momentum k_1 (the incident momentum) or k_2 (the scattered momentum). One may take everything except the denominators, evaluated at these values of q, out of the integral and then integrate over the denominators exactly. This leads to (Maximon 64a)

$$\frac{d\sigma}{d\Omega\, dE_2} = \frac{1}{2\pi}\,\frac{Z^2\alpha^3}{E_1^2 k}\,\{P + B\}\,; \tag{7-26b}$$

the mentioned peak contribution is

$$P = \frac{1}{2}\frac{\cos^2\frac{1}{2}\vartheta}{\sin^4\frac{1}{2}\vartheta}\left\{S(q_2)\left[\frac{E_1^2+(E_2+\omega)^2}{(E_2+\omega)^2}\ln\frac{2E_1}{m_e}-\frac{E_1}{E_2+\omega}\right]\right.$$

$$\left.+\,S(q_1)\left[\frac{E_2^2+(E_1-\omega)^2}{(E_1-\omega)^2}\ln\frac{2E_2}{m_e}-\frac{E_2}{E_1-\omega}\right]\right\}, \qquad (7\text{-}26c)$$

with, cf. Eq. (4-16c):

$$S(q) = \frac{4\pi}{Z^2}\left(\frac{\Delta^2}{q^2}\right)^2\left\{\left[F_C(q)\right]^2+\frac{q^2}{\Delta^2}\left(\frac{1}{2}+\frac{q^2}{\Delta^2}\tan^2\tfrac{1}{2}\vartheta\right)\left[F_T(q)\right]^2\right\}, \qquad (7\text{-}26d)$$

and B is the "background contribution", i.e. the difference between the exact cross section in the high-energy limit and the peaking result, also given explicitly by Maximon. In Eq. (7-26c)*, both terms of order $\ln(E_i/m_e)$ and of order unity were kept, neglecting only terms $\sim (m_e/E_i)^2$ and higher. The background itself is of order unity. The original Schiff approximation retains only the terms $\sim \ln(E_i/m_e)$, which is not a good approximation except at very high energies; for E_i = 30-1000MeV, $\ln(E_i/m_e) \cong 4-8$ only. If it is made anyway and one neglects the transverse form factors, one finds, as expressed by the non-radiative Born cross section $d\sigma(E_1,E_i)/d\Omega$:

---

*which is valid for $E_i \gg m_e$ and for angles not close to zero, i.e. $\vartheta \gg m_e/E_i$. Values of ϑ at or near 180° are permitted: $\pi-\vartheta \lesssim O(m_e/E_2)$; but in this case, part of the background must be retained, so that the peaking approximations itself $(B=0)$ is not valid near $\vartheta=\pi$.

$$\frac{d\sigma}{d\Omega dE_2} = \frac{\alpha}{\pi k}\left[\ln\left(\frac{2E_1}{m_e}\sin\tfrac{1}{2}\vartheta\right) - \tfrac{1}{2}\right]\left\{\left[1+\frac{E_2^{\,2}}{(E_1-\omega)^2}\right]\frac{d\sigma(E_1, E_1-\omega)}{d\Omega}\right.$$

$$\left. + \left[1+\frac{(E_2+\omega)^2}{E_1^{\,2}}\right]\frac{d\sigma(E_2+\omega, E_2)}{d\Omega}\right\};$$

(7-26e)

Nguyen Ngoc (64) however gives

$$\frac{d\sigma}{d\Omega dE_2} = \frac{\alpha}{\pi k}\left\{\left[1+\left(\frac{E_2}{E_1-\omega}\right)^2\right]\ln\frac{2E_2}{m_e} - \frac{E_2}{E_1-\omega}\right\}\frac{d\sigma(E_1, E_1-\omega)}{d\Omega}$$

$$+\frac{\alpha}{\pi k}\left\{\left[1+\left(\frac{E_2+\omega}{E_1}\right)^2\right]\ln\frac{2E_1}{m_e} - \frac{E_2+\omega}{E_1}\right\}\frac{d\sigma(E_2+\omega, E_2)}{d\Omega};$$

see also Hand (63a). (7-26f)

The former expression* is due to Perez y Jorba (61), and goes over into the expression given by Friedman (59) for the elastic case ($\omega = 0$). Eqs. (7-26e, f) have an immediate physical meaning: the first term corresponds to the diagram of Fig. 7.8(b) where the electron is first scattered inelastically by the nucleus and then emits the photon, and the second to Fig. 7.8(a) where the photon is emitted first, so that the electron of energy $E_1 - k = E_2 + \omega$ scatters from the nucleus. Eq. (7-26e) was used frequently by experimenters (Bounin 61, Isabelle 63, Peterson 68), who often employed exact elastic cross sections (obtained

---

*The factors $\sin\frac{1}{2}\vartheta$ were introduced by Schiff (52) ad hoc in order to effect the correct infrared cancellation within the peaking approximation. If background terms are retained as in Eq. (7-26f), this is no longer necessary (Maximon 64a).

by DWBA) rather than Born cross sections for $d\sigma(E_1, E_2)/d\Omega$.

An example of an elastic radiation tail calculation (without magnetic bremsstrahlung) is shown in Fig. 7.12, as obtained from Eq. (7-25e) for ^{9}Be with point charge (dashed curve) and extended charge (solid curves at various values of E_1 and ϑ); the dots are given by the peaking approximation, Eq. (7-26f). The tail is plotted vs. (E_2/E_1) , i.e. as a spectrum of scattered electrons. It is seen that it first decreases from the elastic peak (at $E_2/E_1 = 1$, not shown), but then rises up again for low values of E_2 to form a peak there. This has first been noted by Keiffer (56), who showed that the peak is present only for large angles, $\vartheta \gg m_e/E_1$, and originates from the fact that the coefficient q^{-4} in the cross section which generally is $\sim O(E_1^{-4})$, may become large $\sim O(m_e^{-4})$ for slow emerging electrons, $E_2 \sim m_e$, when also $\underset{\sim}{k} \parallel \underset{\sim}{p}_1$. Eq. (7-26e) explains the large low-energy tail by the fact that in the second term for scattering at low energies E_2 , the Coulomb cross section $d\sigma(E_2+\omega, E_2)/d\Omega$ becomes very large. The two explanations are essentially identical. The figure also shows that the radiation tail gets reduced at larger scattering angles, thus rendering experiments at $\vartheta = 180^\circ$ advantageous, as mentioned earlier.

Fig. 7.13 shows elastic radiation tails for $\vartheta = 180^\circ$ at various values of $T_1 \equiv E_1 - m_e$ plotted vs. T_2/T_1 and normalized by the factor $T_1/(d\sigma^c/d\Omega)$ using Eq. (2-70a), for

a point nucleus without magnetic moment. It is seen that, as T_2/T_1 decreases from the elastic value 1, the tail adjoins the small but non-vanishing* elastic peak, goes through a minimum close to $T_2/T_1 = 1$ and then rises monotonously (for $T_1 \gtrsim 10$MeV) as T_2/T_1 decreases further, as was stated earlier.

The radiation tails of inelastic peaks, as seen e.g. in Fig. 7.5, do not rise for decreasing values of E_2, and are generally smaller than the elastic tail. This is due to the appearance of the inelastic form factors $\bar{F}_C$, $\bar{F}_T$ in Eq. (7-25) which start out as higher powers of q^2 at $q = 0$, see below, and hence negate the effect of the coefficient q^{-4} which would be responsible for the low-energy rise of the tail.

As to the contribution of a magnetic moment to the elastic radiation tail, Fig. 7.14 shows the ratio of point-magnetic to point-charge bremsstrahlung, from Eq. (7-25e) with $F_0^C = 1$, $F_1^M = 1$, plotted vs. ϑ for $E_1 = 54$MeV and $E_2/E_1 = 0.4$, 0.8 and 0.95. The ratio $(\mu/Z)^2(J+1)/3J$ which was taken out of $d\sigma_{mag}$ amounts to 0.0366 in the case of ^{27}Al, e.g. One sees that the magnetic contribution is large near $\vartheta = 180^\circ$ and at energies close to the elastic peak. Fig. 7.15 presents the

---

*The footnote immediately preceding Section 4.4 indicates the value of $V_C(\pi)$, which is finite if m_e is not neglected, so that a small elastic Coulomb cross section remains even at $\vartheta = 180^\circ$.

charge and magnetic contributions for E_1 = 41.5 MeV electrons, elastically scattered at ϑ =180° from ^{7}Li with extended charge distribution (assuming $F_1^M \equiv F_0^C$). The magnetic contribution appears to provide a better joining of the radiation tail to the magnetic elastic peak at $E_2/E_1 = 1$.

Magnetic bremsstrahlung has been directly observed by Goldemberg (Ginsberg 64) in the elastic 180° scattering of 54 MeV electrons from hydrogen, as shown in Fig. 7.16. The dashed curve is the theoretical result for the radiation tail due to a point magnetic moment, which is in fair agreement with the experimental data.

Two points might be added to our discussion of the general bremsstrahlung formula:

(i) If the nuclear continuum states (also known as the "quasielastic peak") are to be studied by inelastic electron scattering, the radiative corrections must be modified. The continuum may be regarded as a summation of many discrete levels, the excitation energy specified by the invariant mass M^*, cf. Eqs. (2-9c), (2-10c). It is convenient to integrate over $(M^*)^2$, and to redefine the previous form factors $F(\Delta^2)$ and $G(\Delta^2)$ by (Tsai 64, Nguyen Ngoc 64, 65, Mo 69)

$$F(\Delta^2)\,\delta(M^{*2} - M^2) \rightarrow F(\Delta^2, M^{*2}), \tag{7-27a}$$

and similarly for $G(\Delta^2)$. In view of Eq. (7-22d), the continuum then just requires the replacement

$$F(\Delta^2) \to \int_{\Delta k}^{k_{max}} F(\Delta^2, M^{*2}) 2(|u| \cos\vartheta_k - u_0) dk \qquad (7\text{-}27b)$$

in Eqs. (7-22a, b), where Δk represents a lower cutoff to the photon energy, corresponding to the cutoff ΔE for the energy resolution in the Schwinger correction. The maximum photon energy k_{max} may be chosen to correspond to the pion threshold of the final state,

$$k_{max} = \frac{1}{2}[u^2 + (M + m_\pi)^2] / (|u| \cos\vartheta_k - u_0), \qquad (7\text{-}27c)$$

and depends on the direction ϑ_k of photon emission.

(ii) For the radiative correction to the elastic proton peaks, one may introduce the proton form factors. This is achieved by comparing Eqs. (7-21d, e) with Eq. (4-4f), with the result

$$N_A N_B G = \frac{1}{4}\Delta^2 |F_{ch}(\Delta^2) + \mu^2 F_m(\Delta^2)|^2, \qquad (7\text{-}27d)$$

$$N_A N_B F = F_{ch}^2(\Delta^2) + \Delta^2 (\mu^2/2m)^2 F_m^2(\Delta^2). \qquad (7\text{-}27e)$$

Mo (69) gives extensive discussions for obtaining radiative corrections to electron-proton scattering; see also Tsai (61), Bartl (66). Experimentally, Tautfest and Panofsky (Tautfest 57) have verified the Schwinger correction in electron-proton scattering at 140 MeV, whereas Allton (64) has also checked the large-angle bremsstrahlung from electrons scattered by protons at

300-500 MeV. Krass (62) has obtained radiative correction formulas for electron-proton scattering if the recoiling proton is observed only.

7.2.7. SMALL-ANGLE BREMSSTRAHLUNG

The radiation tail is influenced by the t^2-effect of small-angle bremsstrahlung from the electron which takes place before or after scattering, while the electron passes a nucleus different from the one which causes the scattering.

The differential radiation probability of electrons of energy E for emitting a photon in ε , $\varepsilon + d\varepsilon$ is given by Rossi (52) or Segrè (53) as

$$\Phi_{rad}(E,\varepsilon)\,d\varepsilon = \frac{F(E,\nu)}{X_0 \ln 183 Z^{-1/3}} \frac{d\nu}{\nu} , \tag{7-28a}$$

per unit length (gm/cm^2), where X_0 is the radiation length,

$$X_0^{-1} = 4\alpha (N/Z) Z^2 (\alpha/m_e) \ln (183 Z^{-1/3}), \tag{7-28b}$$

N = Avogadro's number, and

$$\nu = \varepsilon / E . \tag{7-28c}$$

The function $F(E,\nu)$ depends on the screening parameter

$$\gamma = 100 (m_e/E)[\nu/(1-\nu)] Z^{-1/3} , \tag{7-28d}$$

and has the expressions:

γ = 0 (complete screening),

$$F(E,\nu) = g(\nu) \ln 183 Z^{-1/3} + (1-\nu)/9 , \tag{7-28e}$$

$$\gamma \leq 2, \quad F(E,\nu) \cong g(\nu)\left[\tfrac{1}{4} f(\gamma) + \ln Z^{-1/3}\right],$$

$$2 \leq \gamma \leq 15, \quad F(E,\nu) = g(\nu)\left[\ln\left(\frac{2E}{m_c}\frac{1-\nu}{\nu}\right) - \tfrac{1}{2} - \tau(\gamma)\right], \tag{7-28f}$$

(7-28g)

$\gamma \geq 15$ (no screening),

$$F(E,\nu) = g(\nu)\left[\ln\left(\frac{2E}{m_c}\frac{1-\nu}{\nu}\right) - \frac{1}{2}\right]. \tag{7-28h}$$

Here

$$g(\nu) = 1 + (1-\nu)^2 - (2/3)(1-\nu), \tag{7-28i}$$

and the functions $f(\gamma)$, $\tau(\gamma)$ are tabulated, cf. also Butcher (60). Nguyen Ngoc (65) has given the analytic approximations

$$f(\gamma) = 20.5 - 3.5\gamma + 0.5\gamma^2, \tag{7-28j}$$

$$\tau(\gamma) = (0.613\gamma + 0.93)^{-2}. \tag{7-28k}$$

7.2.8. COLLISION LOSS

The probability that an electron of energy E loses the amount of energy ϵ in a collision with an atomic electron, thereby ionizing the atom, is given by the formula of Møller (32):

$$\Phi_{coll}(E,\varepsilon) = 0.154 \frac{Z}{A}\frac{1}{E^2}\left[\frac{(1-\nu)^2+\nu^2}{\nu(1-\nu)}\right]^2, \tag{7-29}$$

with the coefficient originating from Eq. (7-13d). The corresponding limiting value ξ/ε^2 may be compared to that of the Landau theory, Eqs. (7-14a), (7-15e, g), which is $\xi/(\varepsilon-\varepsilon_0)^2$ for large values of λ. This fact, and the dependence of the folded line shape $I(\lambda, T)$, Eq. (7-19b), on ε through $\lambda = (\varepsilon - \varepsilon_0)/\xi$, suggests that the energies ε be defined with respect to the elastic peak since $\varepsilon_0 \cong \tilde{\varepsilon}$, the most probable energy loss.

7.2.9. CALCULATION OF THE RADIATION TAIL

In order to obtain the complete radiation tail, it is only necessary to add the t^2-contributions Φ_{rad} and Φ_{coll} to the t-contribution of Eq. (7-22a), which we shall designate as $(d\sigma/d\Omega\, dE_2)_t$. The t^2-contributions can be written as (Nguyen Ngoc 65)

$$\left(\frac{d\sigma}{d\Omega\, dE_2}\right)_{t^2} = \frac{1}{2}t\left[\Phi_{rad}(E_1,k) + \Phi_{coll}(E_1,k)\right]\frac{d\sigma(E_1-k,E_2)}{d\Omega} + \frac{1}{2}t\left[\Phi_{rad}(E_2+k,k) + \Phi_{coll}(E_2+k,k)\right]\frac{d\sigma(E_1,E_2+k)}{d\Omega}, \quad (7\text{-}30a)$$

where as in the peaking approximation, the non-radiative scattering cross section $d\sigma(E_1, E_2)/d\Omega$ enters. The first term corresponds to an energy loss k before scattering, the second term to the loss k after scattering. The derivation assumes the scattering to happen at the position $\frac{1}{2}t$, i.e. in the middle of the target, but Bergstrom (67) has shown that the correct folding procedure leads to the same expression, Eq.

(7-30a), to a very good approximation for target thicknesses small compared to one radiation length.

The total radiation tail is then given by

$$\left(\frac{d\sigma}{d\Omega\, dE_2}\right)_{tail} = \left(\frac{d\sigma}{d\Omega\, dE_2}\right)_t C^{-\delta'}\left(\frac{k}{E_1}\right)^{\delta''} + \left(\frac{d\sigma}{d\Omega\, dE_2}\right)_{t^2}, \qquad (7\text{-}30b)$$

where we have added the radiative correction obtained from a differentiation of Eq. (7-11a) with respect to ΔE . The t -term comes from Eq. (7-22a), or else is approximated by Eqs. (7-25a) or (7-25e), or more roughly by Eqs. (7-26e) or (7-26f). Using Eq. (7-22a), Bergstrom (67) has been able to match Eq. (7-30b) to the line shape formula Eq. (7-19c) for ^{12}C within 0.5 to 2.0 MeV from the elastic peak with an accuracy of some per cent. (This satisfies the needed criterion that the procedure should be insensitive to the value of ΔE).

The above refers to the elastic radiation tail. The inelastic tails can be calculated analogously, with e.g. the Schwinger correction taken from Eq. (7-8d).

7.2.10. THE UNFOLDING PROCEDURE

As can be seen from Figs. 7.4, 7.5 and 7.6, the measured spectrum of scattered electrons really represents a continuum consisting of the radiation tails from the elastic and inelastic peaks, and at sufficiently high excitation also of the continuum of nuclear levels with their own radiation tails. For describing this situation, one finally has, using Eqs. (7-19c) and (7-30b), for the observed spectrum:

$$\left(\frac{d\sigma}{d\Omega\, dE_2}\right)_{obs} = \left(\frac{d\sigma}{d\Omega\, dE_2}\right)_{line} + \left(\frac{d\sigma}{d\Omega\, dE_2}\right)_{tail} \qquad (7\text{-}31a)$$

for each level. The continuum however, which cannot be resolved into levels, must be divided into bins of width ΔE_2 , and the lower-lying levels may be regarded as bins themselves. Since the line shape expression $(d\sigma/d\Omega\, dE_2)_{line}$ is so far available for the elastic peak only, cf. Eq. (7-19c), we use the integrated cross sections, i.e. the approximation $(d\sigma/d\Omega)_{level}$ of Eq. (7-16) which holds for both elastic and inelastic peaks (bins), and write for the observed cross section integrated over the nth bin:

$$\int_{\Delta E_2^{(n)}} \left(\frac{d\sigma}{d\Omega\, dE_2}\right)_{obs} dE_2 = \left(\frac{d\sigma}{d\Omega}\right)^{(n)}_{level} + \sum_{m=0}^{n-1} \int_{\Delta E_2^{(m)}} \left(\frac{d\sigma}{d\Omega\, dE_2}\right)_{tail} dE, \qquad (7\text{-}31b)$$

where the interval $\Delta E_2^{(m)}$ is situated at the mth bin. Inspection shows that this represents an integral equation since the tail contributions given by Eq. (7-30b) contain the calculated cross section $d\sigma(E_1, E_2)/d\Omega$ which we wish to extract from Eq. (7-31b), both in $(d\sigma/d\Omega)^{(n)}_{level}$ and in all bins $m < n$ i.e. at a lower incident energy. If the complete expression Eq. (7-22a), or Eqs. (7-25a) of (7-25e) are used rather than the peaking approximation, it is the form factors rather than the cross sections that enter in this way. It is clear that finally to arrive at the "calculated" $d\sigma/d\Omega$ represents a formidable program of unfolding, if it is to be done with sufficient accuracy.

These problems have been discussed by Tsai (64), Isabelle (66a), Crannell (69) and Mo (69), and actual unfolding procedures of experimental data were carried through by Nguyen Ngoc (64), Kendall (64), and Crannell (66). In principle, what must be done is as follows (Crannell 69): Schwinger corrections are first applied to the elastic peak (first bin). The cross section of the second bin is reduced by the amount that comes from electrons that would have been at higher energies had there been no radiative degradation of their energy, and is then subjected to its own Schwinger correction to correct for the electrons that were removed from it. A similar procedure is applied to the third bin, and so on. This iterative procedure can be programmed in a computer.

If one wants to use analytic procedures, one should know all the form factors of the lower-lying levels. This means that the spectra must be measured for a series of different incident energies E_1 at a given scattering angle ϑ (Nguyen Ngoc 64, Kendall 64); the values of the form factors at energies in between may be found by interpolation. First, one Schwinger-corrects the elastic peak and obtains elastic form factors for a sufficient range of q^2. One then calculates the radiation tail of the elastic peak (first bin) and subtracts it from the spectrum. What remains of the first excited peak (second level) is Schwinger-corrected, and the form factors determined; then the radiation tail of the second bin is calculated. This pro-

cedure is then repeated for the following bins.* Since this becomes lengthy for the continuum, an alternate procedure there would consist in assuming a certain shape for the form factors in each bin, calculating its radiative corrections and tail and trying to fit the sum of all this to the observed spectrum.

Finally, it should be kept in mind that first Born approximation forms the basis of most of the corrections discussed in the preceding. For heavy nuclei $Z \gtrsim$ 20-30, exact radiative correction formulas are needed, but are not yet available. If they were, they would probably be so complicated that the above-described unfolding procedure might become well-nigh unmanageable.

7.2.11. RADIATIVE CORRECTIONS FOR MUONS

Intense beams of muons will soon be available at the "meson factories" now under construction. It is often stated that because of their higher mass, radiative corrections to the scattering of muons will be much less than those for electrons, so that the latter may be replaced with advantage by muons as scattering probes of nuclear structure. To clarify this point, Maximon and Tzara (Maximon 68) have compared the ratio ρ between the area of an inelastic peak (at the excitation energy ω), of width ΔE, and the area of the underlying radiation tail in a bin of equal width, as calculated for muon and for

---

*The triangles in Fig. 7.5 represent an example of a corresponding unfolded spectrum.

electron scattering. Assuming $\omega \ll k_1, k_2, q$, thus $q \doteq k_1 - k_2$, they find

$$\varrho_i = \frac{\pi\omega}{4\alpha\Delta E} \frac{e^{-\delta_S(\Delta E)+\delta_S(\omega)} S_{in}(q)/S_{el}(q)}{\frac{m_i^2+\frac{1}{2}q^2}{q(m_i^2+\frac{1}{4}q^2)^{1/2}} \ln\left[\frac{1}{2}\frac{q}{m_i} + \left(1+\frac{1}{4}\frac{q^2}{m_i^2}\right)^{1/2}\right] - \frac{1}{2}} , \quad (7\text{-}32)$$

where $i = e, \mu$; δ_S is the Schwinger correction of Eq. (7-8d), and $S_{el}(q), S_{in}(q)$ is the function of Eq. (7-26d) containing the form factors of the inelastic level, and of the elastic level providing the radiation tail. The ratio ϱ_μ/ϱ_e, approximately obtained by using the denominators of Eq. (7-32) only, is plotted in Fig. 7.17, from which it is seen that solely for small momentum transfers $q \lesssim$ 200 MeV (which are only moderately useful for probing nuclear structure) is it possible to obtain a relative reduction of the radiation tail by a factor $\gtrsim$ 10 when replacing electrons by muons. The planning of muon scattering experiments thus calls for some scrutiny, given that the beam intensities will be smaller than for electrons.

ACKNOWLEDGMENTS

The interest and support of Dr. T. Godlove, Head, Linac Branch, NRL, in the preparation of this report is acknowledged. I am indebted to Professor Hall L. Crannell and Dr. J. Bergstrom, both of Catholic University, for discussions and information.

APPENDIX

A. LIST OF SYMBOLS

E_1 (E_2)	initial (final) total electron energy
$\underset{\sim}{k_1}$ ($\underset{\sim}{k_2}$)	initial (final) electron momentum
θ	scattering angle of electron
$E = E_1 - E_2$	energy transfer
$\underset{\sim}{q} = \underset{\sim}{k_1} - \underset{\sim}{k_2}$	momentum transfer
ω	excitation energy of nuclear level
m_e	electron mass
m	proton mass
M	mass of nucleus
$e_e = -e$	electron charge

B. SUPPLEMENTARY EQUATIONS

Eq. (2-9c) $$E^* = (q^2 + M^{*2})^{1/2}$$

Eq. (2-10c) $$E_{ex} = M^* - M$$

(Eq. 2-12c) $$T = \Delta^2/2M$$
$$= (2k_1^2/M)\sin^2\tfrac{1}{2}\theta\left[1 + (2k_1/M)\sin^2\tfrac{1}{2}\theta\right]^{-1}$$

Hofstadter (57)

Eq. (2-13b) $f_{rec} = \left[1 + (2k_1/M)\sin^2 \frac{1}{2}\vartheta \right]^{-1}$

Eq. (2-20c) $\gamma_\lambda \gamma_\mu + \gamma_\mu \gamma_\lambda = 2\delta_{\lambda\mu}$

Eq. (2-25b) $i\frac{\partial \psi}{\partial t} \equiv H\psi = \left[\underset{\sim}{\alpha} \cdot (\underset{\sim}{p} - e_e \underset{\sim}{A}) + \beta m_e + e_e \Phi \right] \psi$

Rose (61)

Eq. (2-33c) $(\gamma_\mu p_\mu - i m_e)\, u(\underset{\sim}{p}) = 0$

Eq. (2-33d) $\bar{u}(\underset{\sim}{p})(\gamma_\mu p_\mu - i m_e) = 0$

Eq. (2-60a) $d\sigma = (2\pi E_1/k_1)\,\delta(E_1 - E_2 - E)\,\frac{m_e^2}{E_1 E_2}\,|H_c|^2\,\frac{d^3k_2}{(2\pi)^3}$

Eq. (2-70a) $\frac{d\sigma^c}{d\Omega} = \left(\frac{Z\alpha}{2E_1\beta^2 \sin^2 \frac{1}{2}\vartheta} \right)^2 (1 - \beta^2 \sin^2 \tfrac{1}{2}\vartheta)$

Eq. (2-70d) $\frac{d\sigma_R}{d\Omega} = \left(\frac{Z\alpha}{2m_e\beta^2} \right)^2 \frac{1}{\sin^4 \frac{1}{2}\vartheta}$

Eq. (3-3f) $Q_L F_L^C(q) = (4\pi)^{1/2} q^{-L} (2L+1)!!\, \hat{L}^{-1} \hat{J}^{-1} (JJ, L0|J J) \int_0^\infty r^2 j_L(qr) \rho_L^C(r)\, dr$

$(\hat{J} = (2J+1)^{1/2})$

"Uberall (69)

Eq. (3-37b) $j_\mu^p(P', P) = i\epsilon\, \bar{u}(P') \left[\gamma_\mu f_p^{ch}(\Delta^2) + (\mu_p^{an}/2m)\, \sigma_{\mu\nu} \Delta_\nu f_p^{m}(\Delta^2) \right] u(P)$

Yennie (57)

Eq. (3-37c,d) $\frac{1}{\Delta^2} \rightarrow \frac{C(\Delta^2)}{\Delta^2}$, $\quad C(\Delta^2) = \frac{1}{1 + \Delta^2/\Lambda^2}$

Eq. (4-2d) $S_\mu = \bar{u}(k_2)\,\gamma_\mu\,u(k_1)$

Eq. (4-2e) $H_I = -4\pi\alpha\,(S_\mu/\Delta^2)\langle P_2|j_\mu(0)|P_1\rangle\,(2\pi)^3\,\delta(q+P_1-P_2)$

Drell (64)

Eq. (4-3a) $W_{\mu\nu} = (2\pi)^3\,\bar{P}_{10}\hat{J}_i^{-2}\sum_{M_i}\sum_{f}\delta^{(4)}(\Delta+P_1-P_2)\langle P_2|j_\mu(0)|P_2\rangle\langle P_2|j_\nu(0)|P_1\rangle$

Drell (64)

Eq. (4-3c) $W_{\mu\nu} = W_1(\Delta^2,\Delta\cdot P_1)\,(\delta_{\mu\nu}-\Delta_\mu\Delta_\nu/\Delta^2)$

$+W_2(\Delta^2,\Delta\cdot P_1)\,(P_{1\mu}-\Delta_\mu\,\Delta\cdot P_1/\Delta^2)(P_{1\nu}-\Delta_\nu\,\Delta\cdot P_1/\Delta^2)/M^2$

Drell (64)

Eq. (4-3d) $k_1/E_1 \to \left[(k_1\cdot P_1)^2 - m_e^2 M^2\right]^{1/2}/(P_1\cdot E_1)$

Eq. (4-4f)
$$\begin{cases} W_1 = (\Delta^2/4P_{10})\,|F_{ch}(\Delta^2)+\mu^2 F_m(\Delta^2)|^2\,\delta(P_{10}-P_{20}+E), \\ W_2 = (M^2/P_{10})\left[|F_{ch}(\Delta^2)|^2+\Delta^2(\mu^2/2M)^2|F_m(\Delta^2)|^2\right] \\ \qquad\qquad \times\delta(P_{10}-P_{20}+E) \end{cases}$$

Yennie (57a)

Eq. (4-16c)
$$\begin{cases} \dfrac{d\sigma}{d\Omega} = 4\pi\sigma_M^{(1)}\left(\dfrac{\Delta^2}{q^2}\right)^2\left[F_c^2(q)+\dfrac{q^2}{\Delta^2}\left(\dfrac{1}{2}+\dfrac{q^2}{\Delta^2}\tan^2\dfrac{1}{2}\vartheta\right)F_T^2(q)\right] \\ \sigma_M^{(1)} = \dfrac{\alpha^2}{4k_1^2}\,\dfrac{\cos^2\frac{1}{2}\vartheta}{\sin^4\frac{1}{2}\vartheta} \end{cases}$$

Maximon (64a)

Eq. (4-16e) $F_c^2(q) = \hat{J}_i^{-2}\sum_{L=0}|\mathcal{M}_L^{if}(q)|^2$

Eq. (4-16f) $F_T^2(q) = \hat{J}_i^{-2}\sum_{L=1}\left[|\mathcal{T}_L^{E,if}(q)|^2+|\mathcal{T}_L^{M,if}(q)|^2\right]$

Maximon (64a)

Eq. (4-27e) $(1/2m)\, M_L F_L^M(q) = [L/(L+1)]^{1/2} (4\pi)^{1/2} q^{1-L} (2L+1)!!$

$$\times \hat{L}^{-2}\, \hat{J}^{-1} (JJ, L0|JJ) \left\{ (L+1)^{1/2} \int r^2 j_{L-1}(qr) \mu_{LL-1}(r)\, dr \right.$$

$$\left. - L^{1/2} \int r^2 j_{L+1}(qr) \mu_{LL+1}(r)\, dr \right\}$$

"Uberall (69)

REFERENCES

Acker (67) H.L. Acker, and M.E. Rose, Ann. Phys. (New York) 44, 336 (1967).

Akhiezer (65) A.I. Akhiezer, V.B. Berestetskii, Quantum Electrodynamics (Interscience Publishers Inc., New York, 1965).

Allton (64) E.A. Allton, Phys. Rev. 135, B570 (1964).

Bartl (66) A. Bartl and P. Urban, Acta Physica Austriaca 24, 87 (1966).

Baumann (53) K. Baumann, Acta Phys. Austr. 7, 248 (1953).

Berg (58) R.A. Berg and C.N. Lindner, Phys. Rev. 112, 2072 (1958).

Berg (61) R.A. Berg and C.N. Lindner, Nucl. Phys. 26, 259 (1961).

Bergstrom (67) J. Bergstrom, in MIT 1967 Summer Study (Laboratory for Nuclear Science, MIT) 1967, p. 251.

Bethe (34) H.A. Bethe and W. Heitler, Proc. Roy. Soc. A146, 83 (1934).

Bethe (46) H.A. Bethe and J.R. Oppenheimer, Phys. Rev. 70, 451 (1946).

Biel (55) S.J. Biel and E.H.S. Burhop, Proc. Phys. Soc. A68, 165 (1955).

Bjorken (63) J.D. Bjorken, Ann. Phys. (New York) 24, 201 (1963).

Bjorken (65) J.D. Bjorken and S.D. Drell, Relativistic Quantum Mechanics, McGraw-Hill Book Co., New York, 1965.

Bloch (37) F. Bloch and A. Nordsieck, Phys. Rev. 52, 54 (1937).

Blunck (50) O. Blunck and S. Leisegang, Z. Physik 128, 500 (1950).

Blunck (51) O. Blunck and K. Westphal, Z. Physik 130, 641 (1951).

Börsch-Supan (61) W. Börsch-Supan, J. Res. Nat. Bur. Stand. 65B, 245 (1961).

Bounin (61) P. Bounin and G.R. Bishop, J. Phys. Radium 22, 555 (1961).

Braunbek (38) W. Braunbek and E. Weinmann, Z. Physik 110, 360 (1938).

Breuer (65) H. Breuer, Nucl. Inst. Meth. 33, 226 (1965).

Butcher (60) J.C. Butcher and H. Messel, Nucl. Phys. 20, 15 (1960).

Chrétien (55) M. Chrétien, Phys. Rev. 98, 1515 (1955).

Crannell (66) H. Crannell, Phys. Rev. 148, 1107 (1966).

Crannell (69) H. Crannell, Nucl. Inst. Meth. 71, 208 (1969).

Dowling (64) P.J. Dowling, Phys. Rev. 136, B171 (1964).

Drell (52) S.D. Drell, Phys. Rev. 87, 753 (1952).

Drell (64) S.D. Drell and J.D. Walecka, Ann. Phys. 28, 18 (1964).

Elton (52) L.R.B. Elton and H.H. Robertson, Proc. Phys. Soc. A65, 145 (1952).

Elton (55) L.R.B. Elton, Proc. Phys. Soc. A68, 549 (1955).

Eriksson (61) K.E. Eriksson, Nuovo Cimento 19, 1010 (1961).

Friedman (59) J.I. Friedman, Phys. Rev. 116, 1257 (1959).

Ginsberg (64) E.S. Ginsberg and R.H. Pratt, Phys. Rev. 134, B773 (1964).

Goldemberg (66) J. Goldemberg and R.H. Pratt, Rev. Mod. Phys. 38, 311 (1966).

Heitler (54) W. Heitler, The Quantum Theory of Radiation (Oxford University Press, New York, 1954), third edition.

Henry (66) G.R. Henry, Phys. Rev. 149, 1217 (1966).

Hofstadter (57) R. Hofstadter, Ann. Rev. Nuc. Sci. 7, 231 (1957).

Hough (48) P.V.C. Hough, Phys. Rev. 74, 80 (1948).

Hubbard (66) D.F. Hubbard and M.E. Rose, Nucl. Phys. 84, 337 (1966).

Isabelle (63) D.B. Isabelle and G.R. Bishop, Nucl. Phys. 45, 209 (1963).

Isabelle (66) D.B. Isabelle, in Proceed. International School of Physics "Enrico Fermi", Varenna 1965, Course XXXVIII (Academic Press, New York, 1966).

Isaev (59) P.S. Isaev and I.S. Zlatev, Nuovo Cimento 13, 1 (1959).

Isaev (60) P.S. Isaev and I.S. Zlatev, Nucl. Phys. 16, 608 (1960).

Jauch (54) J.M. Jauch and F. Rohrlich, Helv. Phys. Acta 27, 613 (1954).

Jauch (55) J.M. Jauch and F. Rohrlich, Theory of Photons and Electrons, Addison-Wesley Publishing Co., Cambridge, Mass., 1955).

Källén (58) G. Källén, in Encyclopedia of Physics vol 5/1 (Springer Verlag, Berlin, 1958). p. 169

Keiffer (56) D.G. Keiffer and G. Parzen, Phys. Rev. 101, 1244 (1956).

Karplus (50) R. Karplus and N. M. Kroll, Phys. Rev. 77, 536 (1950).

Kendall (64) H.W. Kendall and D. Isabelle, Bull. Am. Phys. Soc. 9, 94 (1964).

Kerimov (61) B.K. Kerimov and I.M. Abutalybov, Sov. J. Nucl. Phys. 5, 107 (1967).

Kinoshita (50) T. Kinoshita, Prog. Theor. Phys. 5, 1045 (1950).

Krass (62) A.S. Krass, Phys. Rev. 125, 2172 (1962).

Kuo (66) P.K. Kuo and D.R. Yennie, Phys. Rev. 146, 1004 (1966).

Landau (44) L. Landau, J. Phys. USSR 8, 201 (1944).

Lomon (56) E.L. Lomon, Nucl. Phys. 1, 101 (1956).

McCormick (56) P.T. McCormick, D.G. Keiffer, and G. Parzen, Phys. Rev. 103, 29 (1956).

Maximon (64) L.C. Maximon and D.B. Isabelle, Phys. Rev. 133, B1344 (1964).

Maximon (64a) L.C. Maximon and D.B. Isabelle, Phys. Rev. 136, B674 (1964).

Maximon (67) L.C. Maximon, in MIT 1967 Summer Study (Laboratory for Nuclear Science, MIT) 1967, p. 240).

Maximon (68) L.C. Maximon and C. Tzara, Phys. Lett. 26B, 201 (1968).

Maximon (69) L.C. Maximon, Revs. Mod. Phys. 41, 193 (1969).

Meister (63) N. Meister and D.R. Yennie, Phys. Rev. 130, 1210 (1963).

Meister (64) N.T. Meister and T.A. Griffy, Phys. Rev. 133, B1032 (1964).

Mitter (54) H. Mitter and P. Urban, Acta Physica Austriaca 8, 356 (1954).

Mittleman (54) M.H. Mittleman, Phys. Rev. 93, 453 (1954).

Mo (69) L.W. Mo and Y.S. Tsai, Revs. Mod. Phys. 41, 205 (1969).

Møller (32) C. Moller, Ann. Phys. 14, 531 (1932).

Motz (64) J.W. Motz, H. Olsen, and H.W. Koch, Rev. Mod. Phys. 36, 881 (1964).

Newton (55) R.G. Newton, Phys. Rev. 97, 1162 (1955).

Newton (55a) R.G. Newton, Phys. Rev. 98, 1514 (1955).

Nguyen Ngoc (64) H. Nguyen-Ngoc and J.P. Perez-y-Jorba, Phys. Rev. 136, B1036 (1964).

Nguyen Ngoc (65) H. Nguyen Ngoc, Ann. Phys. (Paris) 10, 315 (1965).

Onley (70) D.S. Onley, private communication.

Parzen (51) G. Parzen, Phys. Rev. 81, 808 (1951).

Pauli (38) W. Pauli and M. Fierz, Nuovo Cimento 15, 167 (1938).

Perez y Jorba (61) J. Perez y Jorba, J. Phys. Rad. 22, 733 (1961).

Perrin (65) R. Perrin and E.L. Lomon, Ann. Phys. (New York) 33, 328 (1965).

Peterson (68) G.A. Peterson and J. Alster, Phys. Rev. 166, 1136 (1968).

Racah (34) G. Racah, Nuovo Cimento 11, 461 (1934).

Rose (61) M.E. Rose, Relativistic Electron Theory, John Wiley & Sons, Inc., New York, 1961.

Rossi (52) B. Rossi, High Energy Particles (Prentice Hall Inc. Englewood Cliffs, N.J. 1952).

Sarkar (60) S. Sarkar, Nuovo Cimento 15, 686 (1960).

Schiff (52) L.I. Schiff, Phys. Rev. 87, 750 (1952).

Schwinger (48) J. Schwinger, Phys. Rev. 73, 416 (1948).

Schwinger (49) J. Schwinger, Phys. Rev. 75, 898 (1949).

Schwinger (49a) J. Schwinger, Phys. Rev. 76, 790 (1949).

Segre (53) E. Segre (ed.) Experimental Nuclear Physics (John Wiley & Sons Inc. New York 1953).

Sternheimer (52) R.M. Sternheimer, Phys. Rev. 88, 851 (1952).

Suura (55) H. Suura, Phys. Rev. 99, 1020 (1955).

Tautfest (57) G.W. Tautfest and W.K.H. Panofsky, Phys. Rev. 105, 1356 (1957).

Tsai (61) Y.S. Tsai, Phys. Rev. 122, 1898 (1961).

Tsai (64) Y.S. Tsai, in Proceedings of the International Conference on Nuclear Structure, Stanford Univ. (Stanford Univ. Press, 1964)p. 221.

Überall (69) H. Überall and P. Ugincius, Phys. Rev. 178, 1565 (1969).

Ward (50) J.C. Ward, Phys. Rev. 78, 182 (1950).

Williams (29) E.J. Williams, Proc. Roy. Soc. 125, 420 (1929).

Yennie (57) D.R. Yennie and H. Suura, Phys. Rev. 105, 1378 (1957).

Yennie (57a) D.R. Yennie, M.M. Lévy, and D.G. Ravenhall, Rev. Mod. Phys. 29, 144 (1957).

Yennie (61) D.R. Yennie, S.C. Frautschi and H. Suura, Ann. Phys. (New York) 13, 379 (1961).

FIGURE CAPTIONS

Fig. 7.4 Spectrum of 42.6 MeV electrons inelastically scattered from ^{12}C at $\vartheta = 160^{o}$ (left-hand scale). Right-hand scale: elastic peak. Continuous curve: radiation tail. Barber, PRL 3,219(1959)

Fig. 7.5 Spectrum of elastically and inelastically scattered electrons from ^{89}Y, for $E_1 = 70$ MeV and $\vartheta = 130^{o}$ (Peterson 68), showing elastic and inelasti radiation tails.

Fig. 7.6 Spectrum of 70 MeV electrons scattered at $\vartheta = 180^{o}$ from a water target. Points indicate uncorrected data, triangles the data after radiative corrections were applied (Goldemberg 66).

Fig. 7.7 Lowest-order and radiative correction diagrams for electron-nucleus scattering.

Fig. 7.8 Diagrams for photon emission during electron-nucleus scattering.

Fig. 7.9 Transmission Geometry.

Fig. 7.10 Contour for Laplace inversion of Eq. (7-18g)

Fig. 7.11 Cross section correction (line shape) due to Schwinger and straggling corrections for ^{208}Pb, $E_1 = 400$ MeV, $\vartheta = 90^{o}$, $\Delta = 30$ mg/cm^2. Curves include successively Landau, Landau plus radiation straggling, and both stragglings plus Schwinger correction (Bergstrom 67).

Fig. 7.12 Radiation tail from elastic scattering of electrons $E_1 = 150$, 200 MeV ($\vartheta = 60^{o}$, 135^{o}) from ^{9}Be; extended charge (solid curves) and point charge (dashed curve at 200 MeV, 60^{o}). Dots: peaking approximation (Nguyen Ngoc 64).

Fig. 7.13 Radiation tail from $\vartheta = 180^{o}$ elastic scattering from a spinless point nucleus at various values

of $T_1 = E_1 - m_e$ (Motz 64).

Fig. 7.14 Ratio of magnetic to coulomb radiation tail, multiplied with $(Z/M)^2 [3J/(J+1)]$ for $E_1 = 54$ MeV, plotted vs. ϑ at $E_2/E_1 = 0.4$, 0.8 and 0.95 (Ginsberg 64).

Fig. 7.15 Radiation tail of 180° elastic scattering from ^{7}Li, showing charge and magnetic contributions (Ginsberg 64).

Fig. 7.16 Magnetic bremsstrahlung contribution adjoining the elastic peak of 54 MeV electrons scattered at $\vartheta = 180^\circ$ from hydrogen, as observed by Goldemberg (Ginsberg 64).

Fig. 7.17 Ratio of inelastic level areas relative to radiative tails for muon and electron scattering as a function of momentum transfer (Maximon 68).

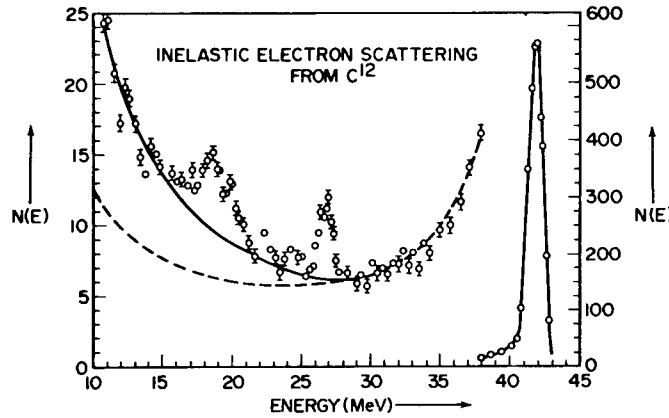

Fig. 7.4 - Spectrum of 42.6 MeV electrons inelastically scattered from ^{12}C at $\vartheta = 160°$ (left-hand scale). Right-hand scale: elastic peak. Continuous curve: radiation tail. Barber, PRL 3,219(1959)

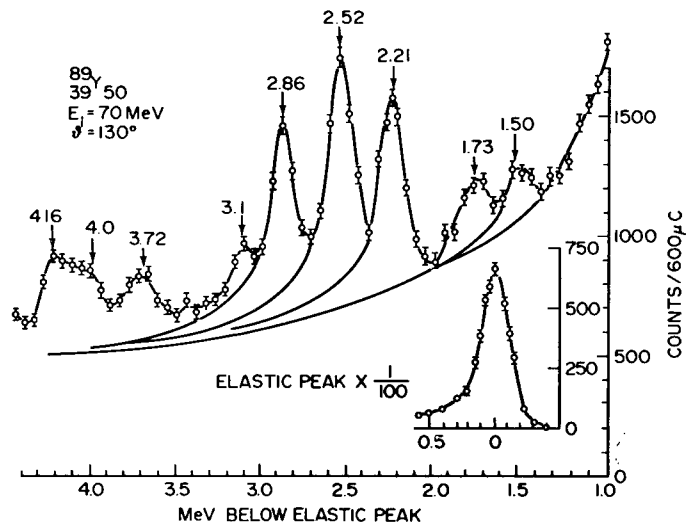

Fig. 7.5 - Spectrum of elastically and inelastically scattered electrons from ^{89}Y, for $E_1 = 70$ MeV and $\vartheta = 130°$ (Peterson 68), showing elastic and inelastic radiation tails

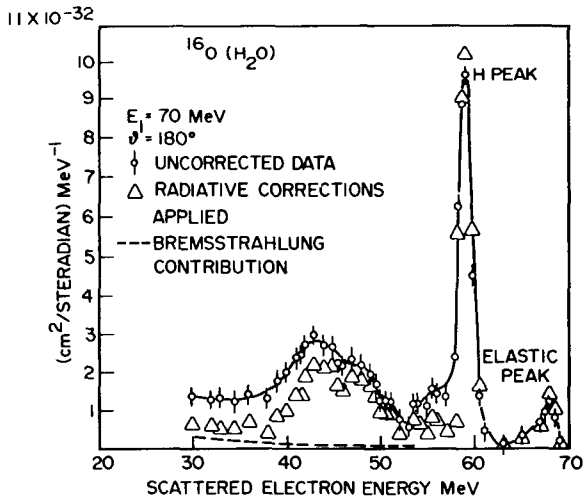

Fig. 7.6 - Spectrum of 70 MeV electrons scattered at $\vartheta = 180°$ from a water target. Points indicate uncorrected data, triangles the data after radiative corrections were applied (Goldemberg 66).

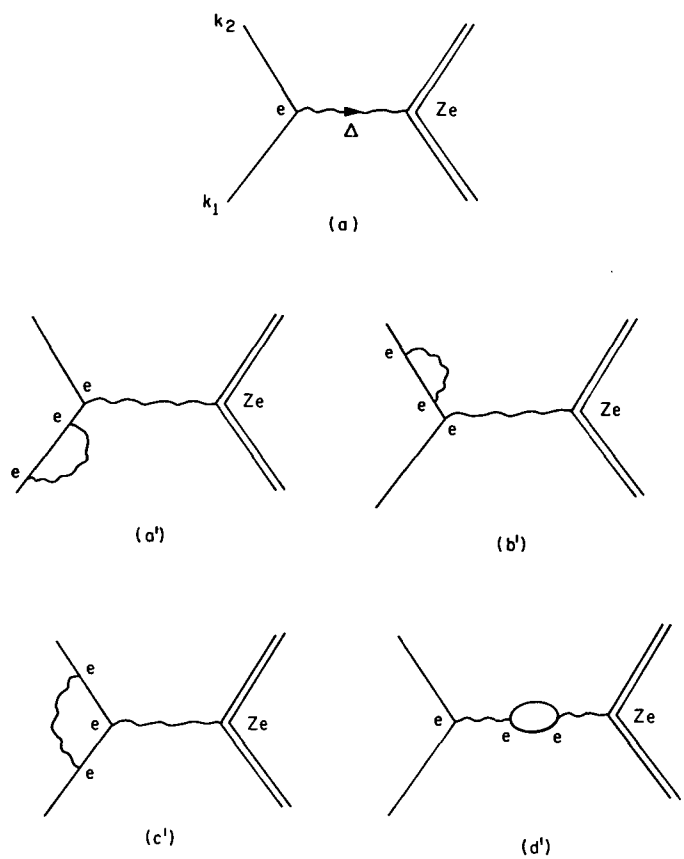

Fig. 7.7 - Lowest-order and radiative correction diagrams for electron-nucleus scattering

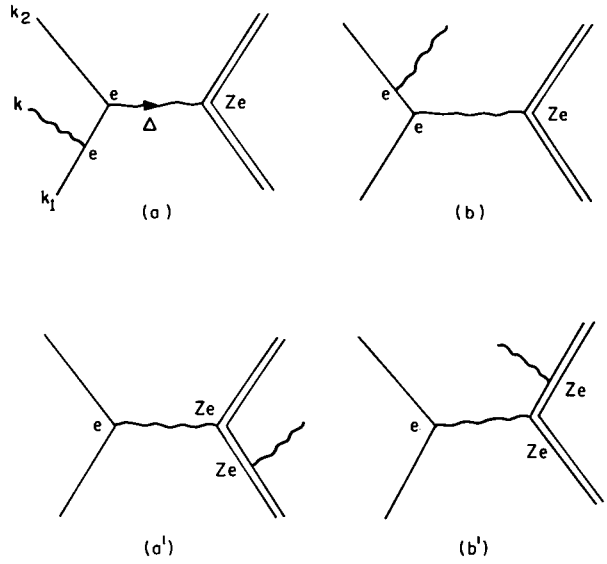

Fig. 7.8 - Diagrams for photon emission during electron-nucleus scattering.

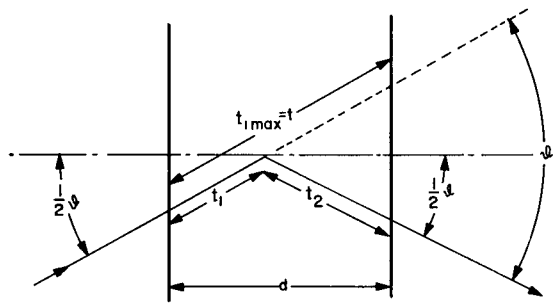

Fig. 7.9 - Transmission Geometry.

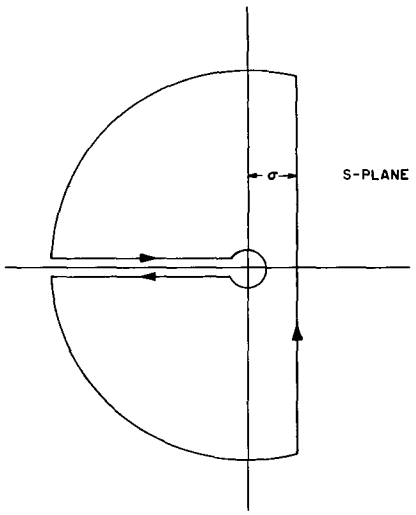

Fig. 7.10 - Contour for Laplace inversion of Eq. (7-18g)

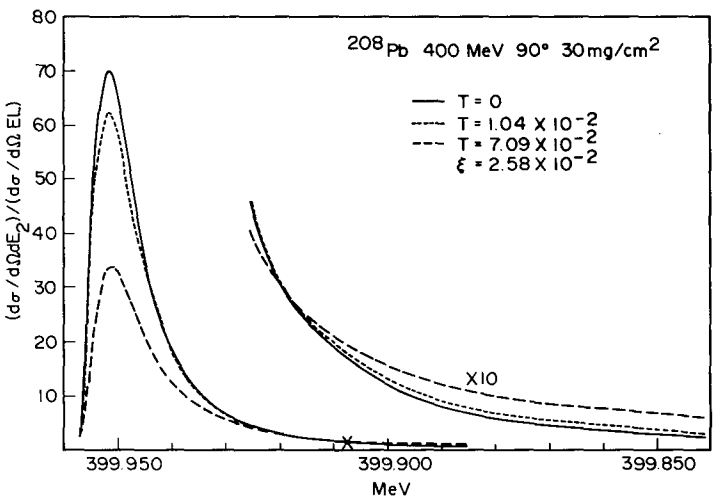

Fig. 7.11 - Cross section correction (line shape) due to Schwinger and straggling corrections for ^{208}Pb, E_1 = 400 MeV, ϑ 90°, d = 30 mg/cm^2. Curves include successively Landau, Landau plus radiation straggling, and both stragglings plus Schwinger correction (Bergstrom 67).

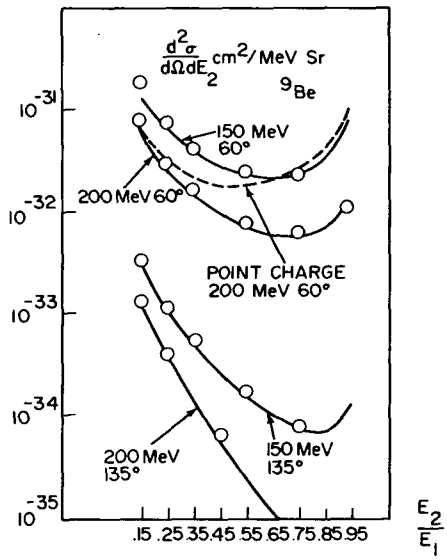

Fig. 7.12 - Radiation tail from elastic scattering of electrons E_1 = 150, 200 MeV (ϑ = 60°, 135°) from ^{9}Be; extended charge (solid curves) and point charge (dashed curve at 200 MeV, 60°). Dots: peaking approximation (Nguyen Ngoc 64).

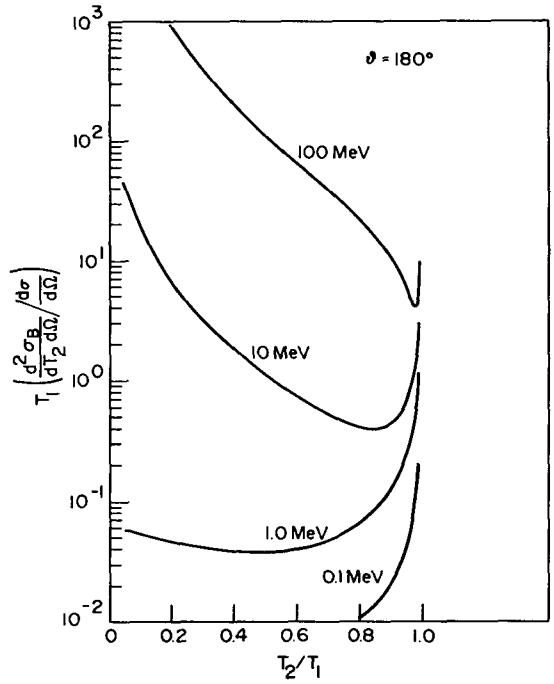

Fig. 7.13 - Radiation tail from ϑ = 180° elastic scattering from a spinless point nucleus at various values of $T_1 = E_1 - m_e$ (Motz 64).

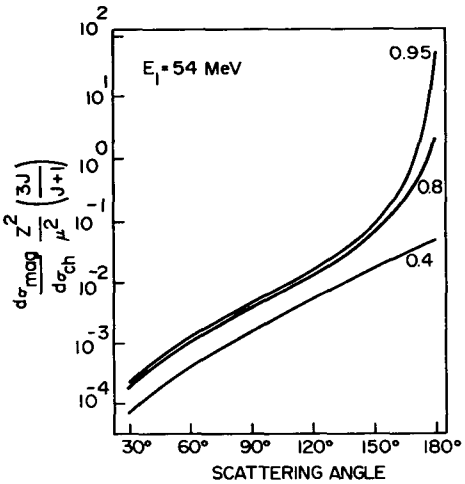

Fig. 7.14 - Ratio of magnetic to Coulomb radiation tail, multiplied with $(Z/\mu)^2$ [3J/(J+1)] for E_1 = 54 MeV, plotted vs. ϑ at E_2/E_1 = 0.4, 0.8 and 0.95 (Ginsberg 64).

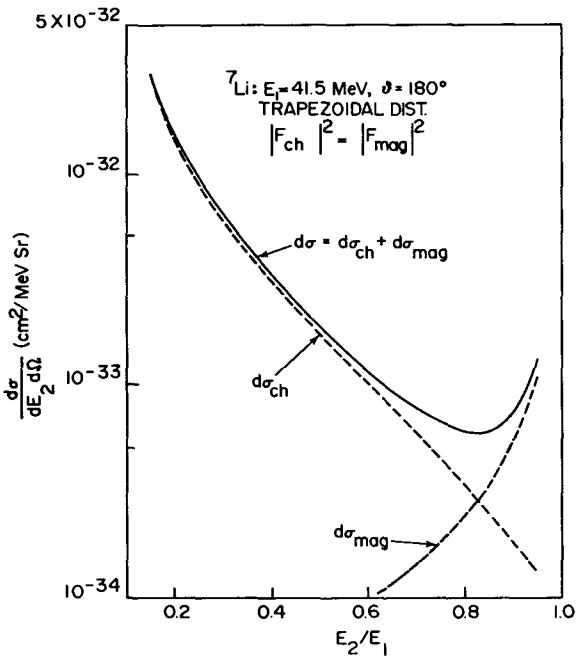

Fig. 7.15 - Radiation tail of 180° elastic scattering from ^{7}Li, showing charge and magnetic contributions (Ginsberg 64).

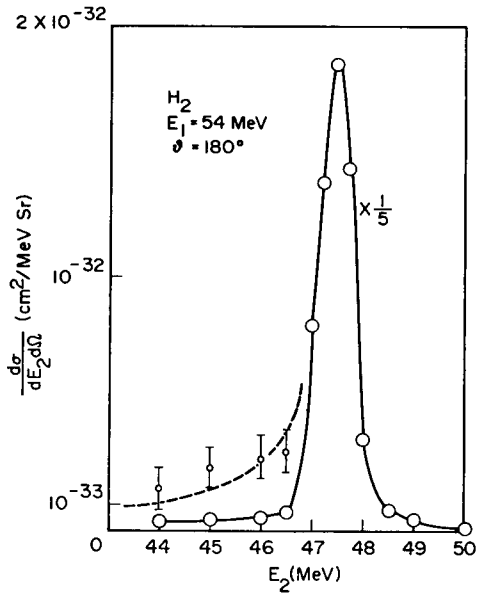

Fig. 7.16 - Magnetic bremsstrahlung contribution adjoining the elastic peak of 54 MeV electrons scattered at $\vartheta = 180^\circ$ from hydrogen, as observed by Goldemberg (Ginsberg 64).

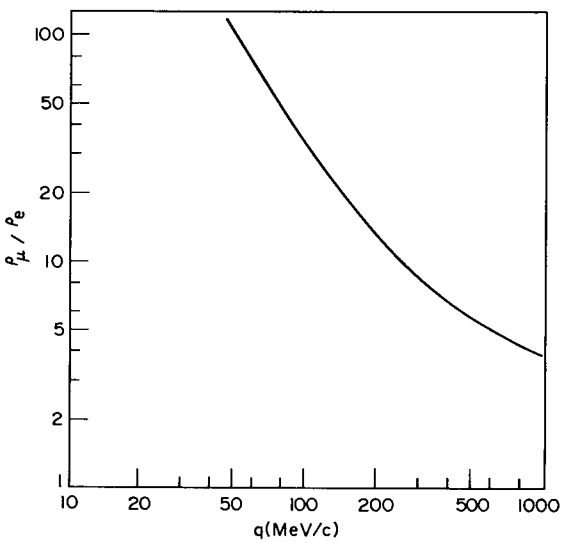

Fig. 7.17 - Ratio of inelastic level areas relative to radiative tails for muon and electron scattering as a function of momentum transfer (Maximon 68).

☆ U.S. GOVERNMENT PRINTING OFFICE: 1970-397-176/135

Security Classification

DOCUMENT CONTROL DATA - R & D

(Security classification of title, body of abstract and indexing annotation must be entered when the overall report is classified)

1. ORIGINATING ACTIVITY (Corporate author)	2a. REPORT SECURITY CLASSIFICATION
U.S. Naval Research Laboratory Washington, D.C. 20390	UNCLASSIFIED 2b. GROUP

3. REPORT TITLE

RADIATIVE CORRECTIONS TO ELECTRON SCATTERING FROM COMPLEX NUCLEI

4. DESCRIPTIVE NOTES (Type of report and inclusive dates)

An interim report on a continuing Problem

5. AUTHOR(S) (First name, middle initial, last name)

H. Uberall (Consultant to NRL Linac Branch; permanent address is The Catholic University, Washington, D.C. 20017)

6. REPORT DATE	7a. TOTAL NO. OF PAGES	7b. NO. OF REFS
May 1, 1970	79	97

8a. CONTRACT OR GRANT NO.	9a. ORIGINATOR'S REPORT NUMBER(S)
NRL Problem H01-09 b. PROJECT NO. RR 002-06-41-5005 c. d.	NRL Report 7080 9b. OTHER REPORT NO(S) (Any other numbers that may be assigned this report)

10. DISTRIBUTION STATEMENT

This document has been approved for public release and sale; its distribution is unlimited

11. SUPPLEMENTARY NOTES	12. SPONSORING MILITARY ACTIVITY
	Department of the Navy (Office of Naval Research), Washington, D.C. 20360

13. ABSTRACT

In this report, we give a review of the present status of radiative corrections to electron scattering from complex nuclei, both from the theoretical standpoint and with a view to practical applications. The first section presents a description of the general features of radiative corrections. The following four sections discuss the individual processes entering into radiative and line shape corrections and their synthesis, while the rest of the report is concerned with individual processes contributing to the radiation tail, and their synthesis (or "unfolding procedure").

DD FORM 1 NOV 65 1473 (PAGE 1)

S/N 0101-807-6801

Security Classification

14. KEY WORDS	LINK A		LINK B		LINK C	
	ROLE	WT	ROLE	WT	ROLE	WT
Nuclear models						
Electron scattering						
Elastic						
Inelastic						
Photonuclear reactions						
Nuclear excited states						
Theory						
Review						